ANL/NSE-21/48

Application of NEAMS Codes to Capture MSR Phenomena

Nuclear Science and Engineering Division

ANL/NSE-21/48

Application of NEAMS Codes to Capture MSR Phenomena

prepared by
Bo Feng, Shayan Shahbazi, Jun Fang, Ting Fei, and Dillon Shaver
Nuclear Science and Engineering Division

08/20/2021

Executive Summary

This report documents work completed in FY21 under the Nuclear Energy Advanced Modeling and Simulation (NEAMS) program's Molten Salt Reactor (MSR) Application Drivers activity at Argonne. The common focus was on identifying the modeling and simulation functional requirements for designing, licensing, and operating MSRs and applying those capabilities already developed in NEAMS tools to example problems of interest. The four main parts of this report each focuses on a specific area of simulation physics as it relates to MSR phenomena: fuel evolution, chemistry, computational fluid dynamics (CFD), and systems analysis.

In terms of fuel evolution, which includes depletion, decay, on-line separations, and transmutation, the current state of computational capabilities for modeling this behavior in liquid-fueled molten salt reactor is discussed. Some of the functional requirements to accomplish the various applications of MSR fuel depletion modeling are highlighted, followed by a summary of recent approaches and code development activities.

The chemistry functional requirements were discussed in the context of several applications of high importance for MSRs, such as corrosion, salt chemistry, and species transport. Each of these types of chemistry modeling have considerable impact on various aspects of reactor applications, including informing on reactor designs, improving operational efficiencies, analyzing safety and reactivity concerns, and estimating the mechanistic source term of the reactor. A brief overview is also provided on code development activities ongoing under NEAMS relevant to chemistry modeling of MSRs.

In terms of CFD applications, the state-of-the-art spectral element code, Nek5000 was used to model the fluid dynamics within a full core of the Molten Salt Fast Reactor (MSFR) concept designed as part of the Euratom EVOL project. This concept was selected as the challenge problem because of its similar features to several U.S. industry concepts. The goal was to model some of the fast MSR design challenges, including potential large internal re-circulations, the need of accurate tracking of delayed neutron precursors (DNP), and the lack of relevant thermal-hydraulics models/correlations, *etc.* Therefore, a series of CFD models were created for the MSFR core cavity using a $k - \tau$ model two-equation model for the turbulence. These first full core results demonstrated that any potential recirculation zones could be properly identified with the current NEAMS CFD capabilities. The development of these models will also set the stage for future testing of Nek5000's functionalities to model other MSR thermal-fluid phenomena.

Lastly, the validation of SAM against experimental data from the Molten Salt Reactor Experiment, which started in FY19, continues with the inclusion of modeling the reactivity insertion tests. This involved using SAM and its point kinetics model for flowing fuel salt to recreate the time dependent power changes and response after positive reactivity insertions at the 1, 5, and 8 MWt power levels. Through these exercises, several code modifications were suggested to the SAM development team and accommodated to enable closer agreement with solid technical and physical justifications. These include adding a moderator reactivity feedback coefficient as an available input and modifying the solution approach for the point kinetics model. Additional SAM development suggestions for flowing fuel MSRs include adding the capability to allow the moderator power change proportionally with the reactor power and enabling specification of the power and DNP distributions separately.

Table of Contents

1 Introduction

The primary goal of the work documented in this report is to apply and assess NEAMS codes for modeling MSR phenomena in thermal and fast MSRs. Unique phenomena of MSRs such as species transport, mass transport, reaction kinetics, delayed neutron precursor drift, recirculation flow in open tank fast MSRs, and others need to be captured in NEAMS codes for design and safety analysis for licensing purposes.

The long term objective is to apply NEAMS chemistry tools (*e.g.*, Mole, MOSCATO, Yellowjacket, *etc.*), thermal fluids tools (*e.g.*, SAM, Nek5000/NekRS, Pronghorn, *etc.*), and neutronics tools (*e.g.*, Griffin) to example models of thermal and fast spectrum MSRs to assess their readiness to capture such phenomena. The end goal is to ensure that these phenomena can be predicted using single-physics codes with the assumed eventual integration of these codes in multiphysics approaches via MOOSE. Some of these fuel evolution and chemistry phenomena that need to be simulated are discussed in Sections 2 and 3, respectively.

Section 4 describes the development of a whole core model of a fast spectrum open tank core MSR via Nek5000 and using it to characterize the flow and temperatures while identifying potential recirculation zones.

Lastly, Section 5 discusses this year's work in validating SAM against a fourth set of transient measurements from the MSRE. Specifically, the reactivity insertion tests were modeled with SAM. This effort resulted in several suggested modifications to the code to improve the physics and agreement, some of which were accommodated this year. This work is part of a larger effort between ANL and ORNL to expand the MSRE transient benchmark, which was initially specified in FY19. With the additional MSRE data (currently export-controlled) from ORNL that was reported to NEAMS in FY20, the NEAMS program can now develop up to 5 MSRE transient test benchmark specifications and potentially refine the previous SAM results using the new information. The goal is to refine and expand the specifications to 4-5 MSRE transient tests and then simulate them using SAM and other codes if needed.

2 Fuel Evolution

The current state of computational capabilities in MSR fuel evolution (depletion, decay, on-line separations, and transmutation) was recently summarized in a report focused on such tools for the purpose of radionuclide inventory calculation for mechanistic source term analysis [1]. Additional applications for these tools include general fuel cycle analyses [2] such as for nuclear material accountancy [3], on-line processing system design [4], or studies on reactor dynamics [5], as well as for isotope harvesting [6] and environmental monitoring [7]. Because nuclear reactors which contain a flowing liquid fuel have the potential for radionuclide distributions outside the primary reactor vessel (*e.g.*, radionuclides can deposit in the heat exchanger or volatilize to the off-gas system), transmutation calculations are not as trivial as those for stationary fuel reactors. Having such a depletion and fuel cycle calculation capability within the NEAMS suite of tools would greatly accommodate the needs from the MSR vendor industry as well as support other DOE-NE work requiring the outputs calculated from this capability. A brief discussion is provided below on the functionalities needed for such a tool.

2.1 Functional Requirements

As mentioned previously, the key difference between flowing fuel and stationary fuel reactors is the potential for continuous or batch removal of certain radionuclides (*i.e.*, certain elements) outside the core (*i.e.*, outside the flux of neutrons). This makes neutronics calculations more challenging as the composition of the irradiated salt in the modeled core changes not only due to transmutation and depletion, but also due to physicochemical considerations specific to the system's salt chemistry, radionuclide deposition phenomena, or off-gas and processing systems. Therefore, a key functional requirement for a tool used to estimate isotopic inventories of an MSR is the ability to remove user-defined amounts of certain elements from the fuel salt at various regions outside the core. The tool should continue tracking fuel depletion and transmutation of the new composition of the fuel salt as it re-enters the core, as well as decay losses and ingrowth throughout the modeled time.

This functionality has a non-negligible impact on the radionuclide inventory in all the applications mentioned above, especially source term analysis and reactor dynamics. Some of the largest yield fission products are short-lived isotopes with half-lives on a similar scale as primary loop residence times. These isotopes eventually beta decay to isotopes of vastly different chemistries. An example includes the sorption of xenon to graphite followed by the beta decay to cesium and either the continued diffusion into graphite or release from it and back into the fuel salt. Alternatively, if xenon stays with the salt as it exits the core, it may release into the off-gas system if stripped out, thereby reducing the cesium content of the salt. This has implications on not only the distribution of the source term of the reactor, but also its reactivity (*i.e.*, Xe-135).

Another example includes the tracking of iodine-131 in MSRs. After the Molten Salt Reactor Experiment (MSRE), analysis of measured samples did not allow for a complete picture of the mass balance of iodine-131 throughout the reactor, possibly due to lower accuracy of the modeling tools used to approximate the inventory of iodine-131. Potential loss pathways include chemical removal from the fuel salt as the parents Sb-131 or Te-131, which is especially likely considering Te has been shown to attack Hastelloy-N with ease. While a fuel depletion and transmutation tool for MSRs should provide the ability to track the isotopic inventory within the

fuel salt, mechanistic source term analyses will benefit from the ability to track the inventory that is chemically removed from fuel salt as well.

Aside from these aforementioned functionalities related to isotopic tracking, a code that can model MSR depletion and its online fuel cycle processes will enable MSR vendors to determine the design parameters for the core and fuel. For example, understanding how the reactivity and compositions change over time will inform on the initial core fissile content and reload fuel salt fissile content. The ability to perform these reactor physics and depletion calculations is essential for an MSR vendor to understand the range of fuel compositions that may be needed and to even demonstrate viability of the reactor and fuel cycle concept.

2.2 Recent Approaches

Unfortunately, different applications of this tool may require different computational approaches due to challenges in finding a compromise between accuracy, timescales, and tractability [8]. Applications involving greater temporal or spatial resolution may need to include an advection term to the depletion model while those such as longer scale fuel cycle simulations may require a more simplified approach [8]. Some examples of recent applications and developments in MSR fuel depletion and transmutation are provided below, although this is not meant to be a comprehensive review.

MSR fuel depletion and transmutation capability development is ongoing in the SCALE suite of codes. A Python script known as TritonMSR was initially developed to complement SCALE/TRITON by handling chemical stream management outside the core using a "semicontinuous batch" approach [9]. Functionalities that TritonMSR introduced include generic geometry modeling, multi-zone and multi-fluid capabilities, time-dependent feed and removal rates, and critical concentration searches. The use of TritonMSR was demonstrated for inventory calculation as it applies to mechanistic source term analysis of both MSRE and Molten Salt Demonstration Reactor (MSDR) [10]. Later, continuous removal and isotope tracking were added into the SCALE/TRITON module and benchmarked against TritonMSR [11]. This was also demonstrated recently by modeling the potential of MSRs to produce Mo-99 [6]. Improved MSR fuel depletion functionality in SCALE/TRITON is planned to be released in the next version, SCALE 6.3 [8].

An extended version of the Monte Carlo neutronics tool Serpent2 has also been used to model MSRs with continuous fission product removal, starting with the Molten Salt Fast Reactor (MSFR) [12]. Similar extensions of the code have been accomplished by others to allow for this functionality of isotope removal/addition from the stationary core model that Serpent2 offers. This includes modeling the whole core of an MSR [13], analyzing the fuel cycle and load following capability of two MSR designs with an external salt processing script [2], and completing an initial source term inventory calculation of three different MSRs with and without potential gaseous fission product removal [14].

Another available tool is the Advanced Dimensional Depletion for Engineering of Reactors (ADDER) software, which is a flexible fuel cycle analysis tool that is meant to be agnostic to the neutronics solver used, and has been demonstrated to be NQA-1 compliant when used with MCNP [15, 16]. The code, written in Python, offers the ability to perform fuel management and

criticality search operations, especially suited for reactors that have complex fuel or material shuffling patterns that persist on various timescales, and development specifically for flowing fuel reactors is ongoing. ADDER has been demonstrated for an MSR design and three different computational approaches within the code were compared [17]. ADDER provides unique functionality for source term tracking in MSRs because it can track different flowpaths and different regions of the primary loop, accounting for spatially defined continuous elemental removal, as well as being able to model different regions of the core itself that may contain different neutronic characteristics.

There is also the possibility of adding built-in depletion solvers to mass transport modeling tools. Recently, a numerical framework for solving depletion in MSRs was developed [18]. Cauchy solvers were shown to be useful for convection-diffusion type problems, and sub-stepping was found to reduce eigenvalues and increase accuracy for certain problem types. Pade and Taylor solvers were also tested and shown to outperform Cauchy solvers in certain cases. All solvers were tested for lumped and 2D depletion. This work demonstrates the ability to implement relatively lightweight depletion modeling frameworks within mass transport and fluid dynamics modeling tools.

According to the latest software development plan for Griffin [19], MSR-specific capabilities will be added in future years. In particular, the development team has identified and prioritized many of the aforementioned functionalities including the ability to model:

- Flowing fuel
- Time-dependent delayed neutron precursor densities (precursor drift)
- Online reprocessing and refueling
- Corrosion
- Structure/reflector feedback
- Radiation heating of reflectors and other in-vessel components
- Cross sections of chloride
- Isotope species tracking (with interactions bubble, off-gas, depositions, etc.)

In particular, the team has also identified MSR-specific transients of interest for simulation:

- ULOF – positive reactivity
- Unprotected single-pump failure in a multi-circuit
  - Control system response time to prevent freezing in heat exchanger
  - Continued operation with one or more failed pumps
  - Core behavior due to inlet flow and temperature asymmetry
- Multi-circuit instabilities and assess impact on stability of core power distribution

3 Chemistry

The role that chemistry plays in molten salt reactors cannot be understated. The corrosion of structural components, the thermophysical and thermochemical properties of various salt mixtures, and the transport of radionuclide species in the primary loop all have strong reliance on understanding various types of underlying chemical phenomena. All of these focus areas of MSR chemistry modeling have a considerable impact on the mechanistic source term (MST) of the reactor, an important part of the licensing pathway for advanced reactors. As discussed in refs [1, 20, 21], chemistry phenomena broadly represent some of the largest information gaps in MSR MST modeling. Additionally, chemistry plays an important role in various aspects of reactor design for operations and maintenance (*e.g.*, corrosion), as well as other aspects of safety analyses. For example, understanding the transport of the noble gas fission product Xe-135 in the primary loop and core graphite of graphite-moderated thermal spectrum MSRs is very important to understanding reactivity effects. But also, understanding the underlying chemistry of bubble transport and noble gas solubility in molten salts, which controls the transport and removal mechanisms from the salt (*e.g.*, gas sparging), is equally as important as the system analysis model which utilizes that information. Therefore, special emphasis should be placed on not just modeling various chemical phenomena of MSRs, but also experimental efforts which will be needed to provide the fundamental data on which the models rely. Chemistry modeling of MSRs is discussed below in the context of the functional requirements for modeling corrosion, salt chemistry, and species transport in MSRs, but it should be noted that these three focus areas are not a comprehensive representation of the full impact of chemistry on MSRs.

3.1 Corrosion

Several NEAMS codes are under development which can capture corrosion related phenomena. Although there are still uncertainties with the underlying physics that control corrosion, several modeling approaches can be taken to simulate leaching and deposition based on various types of experimental data.

First, semi-empirical models, such as those being developed in the engineering scale code Mole, can be deployed to model leaching and deposition of specific elements if the corresponding experimental data exists for that element in that salt and alloy system [22]. This approach results in a less computationally expensive simulation that can be coupled with other relevant phenomena in systems analysis or species transport codes but relies on system-specific experimental data. Similarly, the development of tritium transport models in the SAM code is ongoing to assist in source term analyses but adding capabilities that capture the relationship between tritium content, redox potential of the salt, and the resulting impact on corrosion can help inform on tritium's role in corrosion. Although, corrosion models may not need to be implemented directly into SAM as both MOOSE-based codes SAM and Mole plan to be coupled via the NEAMS Workbench [23]. The role of tritium in corrosion has been studied and discussed extensively, and models have been developed [24]. But given the uncertainties that still exist and the importance of tritium to source term as well as corrosion, more experimentation is needed to fully understand its effect on redox potential in systems of various salt mixtures, fission product concentrations, and alloys.

Second, leaching and deposition can be modeled with thermogalvanic numerical simulations that couple thermal fluids modeling and electron transport mechanisms. It has been shown that thermogalvanic effects play a controlling role with respect to corrosion kinetics. To account for all prevailing corrosion phenomena, additional capabilities would need to be added as well. These include the inclusion of kinetics equations for alloy-salt interactions, coupling the salt simulation to alloy simulations via mapped boundary fields, adding an electron transport equation for conductive solids, and including solid-state diffusion in alloys. The Poisson-Nernst-Planck (PNP) approach combines diffusion-based mass transport (Fickian) with an additional migration term dependent on the electric potential of the system and maintains electroneutrality in a computational fluid dynamics framework [25]. Reaction kinetics are controlled by surface fluxes of the species that are the result of electrochemical reactions at the interface. These are modeled with a relationship of the local current density as a function of electrode potentials. Modeling corrosion with this method adds a level of fidelity to typical corrosion modeling approaches but is more computationally expensive, although it may require less demanding experimental data. The diffusion coefficients, found experimentally, are specific to the element in that salt and alloy system but do not need to be found for systems of different geometries or flow parameters.

An important aspect of corrosion modeling is thermochemical modeling of the salt as well as the alloy. The Molten Salt Thermal Properties Database – Thermochemical (MSTDB-TC) is being developed to supply the necessary thermodynamic information to a Gibbs energy minimization solver (*e.g.*, Yellowjacket or Thermochimica) which can calculate chemical and phase equilibria in a molten salt mixture [26]. Such a database is needed to accurately model fission and corrosion product speciation in the salt due to the non-ideal behavior of molten salts [27]. The thermodynamic data stored in the database are those derived from experimental data and typically found with various methods of thermal analysis of the corresponding salt system. Larger, more complex salt systems can be represented with thermodynamic data of the pseudobinary sub-systems by using the modified quasichemical model. But this still requires a large amount of corresponding experimental data to be found, *i.e.*, the pseudobinaries for every component paired with every other component in the modeled mixture.

In addition to a GEM solver for thermochemical equilibria calculations, the Yellowjacket code will also contain phase field microscale corrosion modeling which couples charge transport, heat transport, and mechanics. The coupled equations are solved with finite element modeling and based on the MOOSE framework to facilitate coupling with other NEAMS codes such as Grizzly and Mole.

Finally, there may be additional phenomena worth investigating that may not necessarily be captured by models in the above codes. For example, it is understood that the build-up of fission products has a net oxidizing effect on the fuel salt, but a modeling tool which quantifies this build-up in terms of redox potential of the salt and its impact on corrosion has yet to be seen. Similarly, a model which captures the relationship between impurity levels and corrosion may be useful for unfueled coolant salts.

One specific phenomenon that was found during the MSRE is the intergranular cracking of INOR-8 alloy [28]. The mechanism of crack formation needs to be clarified, and there is a need for models developed for this specific type of corrosion of some nickel-based alloys in molten fluoride salts. This is especially important because large concentrations of the fission product

tellurium were found in the corroded alloy, and tellurium represents an important radioisotope as tracking its iodine daughter is important to mechanistic source term analyses.

Another phenomenon that needs further experimental investigation is the effect of irradiation on corrosion. Recent studies have shown that proton irradiation decelerated intergranular corrosion of Ni-Cr alloys in molten salts [29]. It is unclear if neutron irradiation will have the same effect, but additional experiments are warranted. Models accounting for this phenomenon should also be developed in corrosion modeling tools but coupling these tools to reactor physics tools may be necessary to properly account for the type and magnitude of radiation. This provides yet another example of the importance of multiphysics experimental investigations. A natural circulation molten salt loop of fuel-bearing salt in a neutron irradiation environment is planned and will hopefully result in irradiated corrosion experimental data [30].

3.2 Salt Chemistry

Accurate speciation of fission products and actinides in molten salt systems depends heavily on thermochemical modeling. While speciation of ideal chemical systems just depends on a minimization of the Gibbs free energy of the system's components, this is not so trivial for molten salt systems due to the strong non-ideal behavior of many ionic systems like salts. The effects of non-ideality can be simply described by either a negative or positive deviation from ideality. Put simply, a solute dissolved in a molten salt solution which experiences a negative deviation will result in that solute being more stabilized in the solution, and thus will have a lower vapor pressure than it would have as a pure component at that temperature. A positive deviation from ideality will result in the solute being destabilized in the solution relative to how it would behave as a pure component in that environment, and thus will have a vapor pressure higher than its pure component value. These equate to a solute's negative deviation from ideality having an activity coefficient below 1 and a positive deviation result in an activity coefficient above 1.

A literature review of thermochemical modeling in molten salts as it applies to radionuclide speciation was recently completed, so a complete review is omitted here [27]. The recommended computational model for molten salt systems is the modified quasichemical model (MQM) with the two sublattice quadruplet approximation (TSQA) [31]. This complex computational formalism simplifies the types of experimental data needed but does not sacrifice fidelity in the model. At minimum, MQM requires pseudobinary thermodynamic data for pairs of endmembers of the desired salt mixture to be modeled. For example, when modeling the LiF-BeF_2-UF_4 system, the modeler would need experimental data (*e.g.*, phase diagram data) for the LiF-BeF_2, LiF-UF_4, and BeF_2-UF_4 pseudobinary systems. The benefits of this approach are realized as the molten salt systems increase in complexity, *i.e.*, modeling the behavior of a mixture with a multitude of fission products, each representing an endmember.

The model utilizes this experimental data in the form of pair interaction terms. These parameters are determined by optimizing and fitting the model to the experimental data and can be time consuming if the phase diagram for that pseudobinary system is complex. Utilizing some form of experimental data is nonetheless necessary to be able to account for non-ideal effects. Optimizing pair interaction terms for every possible combination of every pair of endmembers may not be necessary for fueled molten salt mixtures as fission products may only have base salt components as first and second nearest neighbors. Therefore, it may be advisable to only measure

experimental data and optimize pair interaction terms for each fission product with each base salt component (*e.g.*, the LiF-CsF and CsF-BeF_2 systems may be sufficient for modeling Cs in the LiF-BeF_2 salt system).

Currently, the commercial software FactSage has been developed over the past two decades by the developers of MQM for various material types but the included data for molten salt systems relevant to nuclear reactors is incomplete. Under the NEAMS program, the Molten Salt Thermal Properties Database – Thermochemical (MSTDB-TC), which is also based on MQM, is being developed specifically with nuclear molten salt systems in mind [32, 33]. Thermodynamic data are provided for both common fluoride and chloride salt system components, and it will eventually include all relevant corrosion and fission product elements. It should be noted that not all fission products are salt soluble, therefore while they can still be modeled in the phase and chemical equilibria calculations, they will not be represented in the solution model, *i.e.*, they will not have interaction terms representing non-ideal behavior as solutes dissolved in solution.

The calculation of phase and chemical equilibria is accomplished with a Gibbs energy minimization (GEM) solver. The types of GEM solvers have been covered extensively elsewhere in literature, but it is noted here that the Thermochimica solver has been developed to be used with thermodynamic data provided by either FactSage or MSTDB-TC [34, 35]. Another GEM solver similar to Thermochimica is currently being developed called Yellowjacket but will be built on the MOOSE framework to facilitate multiphysics coupling. Specifically, Yellowjacket will contain two functionalities built-in: a GEM solver for use with a thermodynamic database like MSTDB-TC and a phase field microscale corrosion modeling tool which will couple charge transport, mechanics, and heat transport for use in molten salt systems [36].

Finally, because MSRs are liquid fueled reactors, the need for accurate thermophysical properties of molten salts is of paramount importance as such properties have significant impact not only on the accuracy of fluid dynamics modeling but also reactor physics, source term, and structural mechanics. Advances in methods in computational chemistry such as density functional theory and machine learning algorithms utilizing neural networks offer the possibility of property prediction but often require considerable human or computational resources and have mostly been applied to simple salt systems. Ultimately, properties for many types of molten salt mixtures will need to be experimentally found, which also requires considerable resources. Nonetheless, the impact of thermophysical properties on nearly every aspect of reactor design and safety analysis motivates research from both approaches in parallel. Additionally, recent planning for a natural circulation molten salt flow loop will aim to provide data on thermophysical property monitoring for a fuel-bearing salt in an irradiation environment [30].

In summary, salt chemistry plays a large role in fission product and actinide speciation and solubility which has a direct role in source term modeling, reactivity/criticality calculations, species transport, and corrosion modeling. Similarly, accurate thermophysical properties are needed in almost all aspects of reactor analysis and motivate continued experimental measurements and technique development as well as novel computational methods of prediction.

3.3 Species Transport

Species transport modeling has many applications including modeling the impact of certain fission products on reactivity [2, 37], the impact of certain salt components on redox control, and

thus corrosion [22, 25], and impact on source term of the transport of various phases containing radionuclides (*e.g.*, salt, bubble, aerosol, *etc.*) [30, 38, 39], especially including the transport of tritium [24]. A brief discussion is provided below on several applications of species transport modeling and the functionalities needed for the type of simulation.

3.3.1 Impact on Reactivity

Species transport within MSRs has an impact on the reactivity or criticality of the reactor. Spatial and temporal modeling of the transport of certain fission products within the core as well as throughout the primary loop is very important to reactor safety. For example, Xe-135 represents an important fission product to all nuclear fission systems, as its very large thermal neutron absorption cross section makes it a strong poison in the reactor. While solid fueled reactors can conservatively assume homogeneous distribution of fission products throughout the fuel, liquid fueled reactors must incorporate system-specific information in the reactor physics analysis to accurately model the transport and distribution of this isotope throughout the core and salt.

During the MSRE, a model was developed for Xe-135 migration, accounting for generation, decay, burnup, stripping, and migration to graphite and circulating bubbles [40]. A revisiting of these phenomena and the incorporation of the resulting models in modern tools has been reported recently and continued development in other tools is recommended [41, 42]. Multiple approaches can be imagined, including accounting for these phenomena in reactor multiphysics tools such as Griffin, or adding these chemical transport models to system analysis tools such as SAM which have modified point kinetics under development [43].

The importance of modeling removal rates of Xe-135 on the reactivity and fuel lifetime of several thermal spectrum fluoride salt reactors was recently shown [37]. Even at low efficiencies of the off-gas stripper system, there was considerable impact of removing Xe-135 on fuel salt lifetime, utilization, and reactivity. These analyses were completed with new feed and removal capabilities within SCALE/TRITON but can conceivably be modeled within other fuel depletion and transmutation tools under development for MSRs as well (See Section 2).

Similarly, the importance of Xe-135 on load-following ability of MSRs was shown recently [2]. The time dependence of the concentration of not only Xe-135, but also its parent I-135, plays a critical role in the ability for MSRs to load-follow (*i.e.*, ramp up power quickly from a shutdown state). For thermal spectrum reactors, load-following capability benefits greatly from on-line removal of Xe-135, while MSRs with harder spectrums may have an easier time load-following due to the lower absorption cross section of Xe-135 at higher energies. Adding a species transport model within such neutronics analysis tools may continue to refine the results and elucidate additional phenomena important to the load-following capability of MSRs. For example, the spatial distribution of Xe-135 in the core (*e.g.*, diffusion into graphite, bubble entrainment, *etc.*) should also be investigated for the impact on load-following capability as well as other reactivity effects.

3.3.2 Impact on Corrosion

Although a summary of corrosion modeling approaches was already provided above, it should be noted that species transport modeling has an impact on corrosion as well, and therefore incorporating this physics in corrosion modeling codes may provide new insights. Understanding

interactions at the salt-alloy interface is vital to simulating corrosion but modeling the flow of electrochemically sensitive elements within the primary loop adds a level of fidelity in terms of the distribution of leached structural components and deposited salt components.

This can be seen in thermogalvanic models of molten salt systems, which provide a framework that accounts for the relationship between heat and electron transport. In a static system, maintaining the constraints of electroneutrality and conservation of heat may be simpler to simulate as there may not necessarily be temperature gradients. But with flowing salt systems with various temperature gradients depending on the region of the loop, this can have a considerable impact on the transport of electrons (*i.e.*, redox reactions) at that specific salt-alloy interface. For example, a simulation of Cr leaching and deposition in a natural circulation loop containing a $MgCl_2$-KCl-NaCl salt showed that the hotter region of the loop resulted in more corrosion/leaching of Cr from the alloy, which was deposited across various colder regions of the loop, dependent on the bulk flow and concentration of the Cr species [25]. This functionality adds fidelity to the simulation by providing the modeler a greater understanding of the distribution of corrosion across loops and systems of arbitrary geometry.

Similarly, the engineering scale MOOSE-based molten salt species transport code Mole is being developed for mass accountancy modeling in flowing liquid and will include a wide variety of phenomena such as movement of species around the primary loop, leaching from system components into the fluid, deposition onto system components, gas bubble formation, and transport of species between gas bubbles and the fluid. The code's advection solvers are utilized to track species transport, and Arrhenius-type relationships are used to model semi-empirical corrosion and deposition models for various species between the salt and alloy. This has been demonstrated for Cr loss from NiCr alloys in KCl-$MgCl_2$ salt mixtures, and the mass distribution of Cr across a sample loop shows the impact of species transport on corrosion [22].

Both codes demonstrate the need for species transport functionality within corrosion modeling tools, but the reliance of both tools on experimental data should be reiterated. Although corrosion phenomenology is not completely understood, it is clear that corrosion simulations should be able to handle species transport coupled with the salt-alloy interaction model due to the strong dependence of the phenomenon on temperature and concentration of key species. This is especially demonstrated in studies that focused on tritium transport, where codes have been formulated to model the impact of tritium on the redox potential, and thus corrosion [24].

3.3.3 Impact on Source Term

The impact of species transport modeling in MSRs on the mechanistic source term of the reactor has been summarized elsewhere [1], but some examples are provided here. The importance of species transport to source term is demonstrated by the fact that radioactive fission, corrosion, and activation products cover a wide range of chemistries in the reactor, and therefore spatial and temporal resolution of the distribution of each chemical group of radionuclides is needed to begin to model the mechanistic source term of the reactor.

Multiple efforts in modeling radionuclide transport in single or multi-phase flows have been reported recently [38, 39, 41, 44-46]. Ultimately, more experimental work needs to be completed to refine the phenomenology of radionuclide transport in molten salt flows, including but not limited to bubble entrainment and transport, aerosol modeling, deposition on solid components,

adsorption and diffusion through graphite, and a better understanding of noble metal transport. During MSRE, several elements were lumped together and classified as "noble metals", but a better classification is needed, as Te, Ag, and Mo all have unique salt chemistries, for example. As the necessary experimental thermodynamic data is optimized and added to MSTDB-TC, a coupling of this database to the GEM solver (*e.g.*, Yellowjacket) and species transport modeling tool (*e.g.*, Mole) will provide more insight into the various behaviors of these radionuclides.

As the modeling tools develop, there will be a need for validation data. While documentation from the MSRE provides some data to compare to, uncertainties are often not reported and inconsistencies in reported results are not uncommon. A modernization and digitization of certain types of MSRE data is under development, as will be discussed in the next section for fission product behavior. Nonetheless, validation data derived from modern experiments and measuring tools will still be needed. An example is seen by the ongoing planning for a fuel-bearing molten salt loop to be irradiated in the Advanced Test Reactor (ATR) [30]. This will hopefully provide the necessary experimental data on noble metal and bubble transport and how it impacts source term assessments and other applications of fission product transport in molten salts.

Another example of the need for species transport modeling on source term modeling is tracking tritium [47]. Understanding the magnitude and chemical form of tritium releases from nuclear reactors is important to dose consequence models. For MSRs, this analysis requires accounting for similar phenomena as that done for LWRs, including but not limited to speciation, diffusion through alloys (*e.g.*, heat exchanger materials), and sorption and trapping in materials (*e.g.*, graphite). But also, these tritium-specific models must be coupled with species transport and tritium generation models to fully account for the nature of radionuclide transport in MSRs. Development of tritium transport models in the SAM code has been ongoing for the fluoride salt-cooled high temperature reactor, but the functionalities developed apply to some MSR designs as well [48].

3.4 Data from the Molten Salt Reactor Experiment

A recent effort was undertaken [49] to digitize the tabulated data in the report "Fission Product Behavior in the MSRE" [50]. This data, in the form of a spreadsheet, will be released along with other types of digitized data from MSRE reports in a publicly available distribution. Examples of the types of data digitized include radiochemical measurement data from various types of samples pulled from the pump bowl of the reactor including liquid salt samples, gas samples, and graphite and metal deposition specimens, as well as graphite and metal surveillance specimens inserted in the MSRE graphite core, specimens and components from the off-gas system, and post-mortem analyses of various reactor system components. Isotopes measured include (but not limited to) Sr-89, Sr-90, Y-91, Ba-140, Cs-137, Ce-144, Zr-95, Nb-95, Mo-99, Ru-103, Ru-106, Sb-125, Te-132, and I-131, as well as chemical analyses of base salt components Li, Be, Zr, and U. Although uncertainties are often not reported, the data represents the only substantial database of information that provides insights on fission product behavior in molten salt reactors that were operated.

4 Computational Fluid Dynamics

Under the DOE's Nuclear Energy Advanced Modeling and Simulation (NEAMS) program, cutting-edge Computational Fluid Dynamics (CFD) techniques are being developed to support the design efforts of the next generation of nuclear power plants. Multiple unique technologies have been proposed which promise to deliver revolutionary amounts of carbon-free electricity with inherently safe designs. One such technology is the molten salt reactor (MSR) [51]. Note that the MSR here refers to the reactors that utilize the molten salt as both the coolant and the fuel, which differentiates itself from reactors that only use the molten salt as the coolant, such as the Fluoride-salt-cooled High temperature Reactors (FHR). In MSRs, the molten salt involved is typically chloride or fluoride based. Since the MSR fuel is in the liquid state, this represents a significantly different paradigm compared to traditional light water reactors (LWR) which use solid fuel rods. As a result, the melting point of the fuel is no longer a limiting factor in the reactor design, completely eliminating a major safety concern. However, this brings its own set of challenges. A key focus of the NEAMS program has been in the development of modeling and simulation capabilities to address these challenges.

The capabilities being developed by the NEAMS program cover a wide range of physics, including materials, structural mechanics, fuel performance, neutronics and CFD. One of the primary needs in the modeling and simulation of MSRs is the development of CFD capabilities. Traditionally, CFD has been used in the simulation of the reactor coolant [52]. In MSRs, the molten salt acts as both the fuel and the coolant, enhancing the importance of accurate thermal-hydraulic analyses. The flow physics expected in an MSR core represent a new set of challenges which have only begun to be explored, even at moderate computational scales. The current study aims to investigate these novel flow physics to gain insight into the overall effects on the full core and provide references to lower-fidelity modeling approaches commonly used in actual reactor design efforts.

The fact that the molten salt serving as both the fuel and the coolant causes any recirculation zones present in the reactor core to become a principal concern. These recirculation zones have a higher chance of appearing in fast spectrum MSR cores that have unrestricted fuel flow through a large core cavity as opposed to coolant channels in conventional thermal MSRs [53, 54]. The molten salt is heated volumetrically and the effects of advection are relied on to remove the generated heat. In a recirculation zone, the same fluid 'parcel' remains trapped and continues heating with only conduction to cool it. Due to the low thermal conductivity associated with molten salts, conduction is a poor heat transfer mechanism and recirculation zones have the potential to reach significantly high temperatures and damage the surrounding structural materials and reactor vessel. A high-fidelity turbulence model, such as the large eddy simulation (LES) present in Nek5000, can help accurately predict where these zones may occur. An additional issue for MSRs with unrestricted flow is the need to track delayed neutron precursors [55]. These are the fission products that release neutrons through radioactive decay a few seconds or minutes after the initial fission reaction rather than immediately through the fission reaction like prompt neutrons. The operation of nuclear reactors is impossible without these delayed neutrons contributing a small fraction to the controlled chain reactions. In conventional solid fuel, these delayed neutron precursors always stay in the fuel, so they are easy to track, but for MSRs the precursors flow with the fuel outside of the core through the heat exchanger loops and back in. Therefore, their sometimes complex flow pathways need to be accurately tracked via CFD for proper accounting of the delayed neutron contributions.

Meanwhile, another challenge associated with MSRs is the high Prandtl number typical of molten salts. The Prandtl number is a property of a fluid representing the ratio of its momentum diffusivity to its thermal diffusivity and plays an important role in heat transfer. In the fluids common for a typical CFD analysis, the Prandtl number is of the order of unity and many of the ubiquitous models used in CFD have been developed for these conditions. It is well known from experiments and high-fidelity simulations of liquid metals, that these relationships do not hold for low-Prandtl number fluids and it is expected that the same is true for high-Prandtl number fluids. An investigation using a high-fidelity method has shown that the NEAMS tool Nek5000 [56] is able to capture these effects.

The current study focuses on demonstrating the readiness and flexibility of NEAMS CFD capabilities in addressing the MSR related design needs. A series of numerical simulations were conducted based on the MSR models available in public literature. Specifically, the reactor model considered herein is based upon the Molten Salt Fast Reactor (MSFR) design proposed under the Euratom EVOL (Evaluation and Viability of Liquid Fuel Fast Reactor Systems) project [57]. The MSFR is a fast breeder reactor with large negative temperature and void reactivity coefficients, offering unique safety characteristics not found in solid-fuel fast reactors. This reference MSFR is a 3000 MW fast-spectrum reactor with three different circuits: the fuel circuit, the intermediate circuit, and the power conversion system. In the fuel circuit, there are 16 sets of pumps and heat exchangers around the core. Representative 2-D axisymmetric and 3-D full core CFD models are created for the MSFR core cavity region using Nek5000. Leveraging the existing MSFR studies available in literature, the "Geometry II" model investigated by Rouch *et al.* [57] was selected as the reference geometry for our CFD simulations. The CFD solver, turbulence models, and detailed simulation case setups are presented in the following sections.

4.1 Numerical Method

Nek5000 is an open source CFD code based on the spectral element method (SEM) [58] with a long history of use in reactor thermal–hydraulics research [52]. SEM combines the accuracy of spectral methods with the domain flexibility of the finite element method. In Nek5000 calculations, the domain is discretized into E curvilinear hexahedral elements, in which the solution is represented as a tensor product of N^{th}-order Lagrange polynomials based on the Gauss–Lobatto-Legendre (GLL) nodal points, leading to a total number of grid points $n = EN^3$. Nek5000 was designed from the outset to take advantage of distributed-memory platforms. It is highly parallel and has been previously applied to a wide range of problems to gain unprecedented insight into the physics of turbulence in complex flows [52]. The time-stepping scheme of Nek5000 is semi-implicit: the diffusion terms of the Navier-Stokes equations are treated implicitly by using a k^{th}-order backward difference formula (*BDFk*), while nonlinear terms are approximated by a k^{th}-order extrapolation (*EXTk*) [59]. Nek5000 was originally developed for simulating turbulent flows with very high fidelity, *i.e.*, DNS and LES. More recently, the RANS capability was implemented in the form of the regularized $k - \omega$ models and the $k - \tau$ model [60-62]. Both LES and DNS require proper resolution of turbulent length scales, which can be very expensive computationally. Considering the problem size involved in MSR core flow simulations, the RANS model would be the most practical option. Nevertheless, LES also plays an essential role in this study, which will be applied in the full core model at a relatively low Reynolds number and generates much needed reference data to evaluate/calibrate the RANS approach. The combination of RANS and LES forms a flexible strategy that balances both the efficiency and the accuracy.

Continuous validation and verification studies have been conducted over years for Nek5000 for various geometries of interest to nuclear engineers, such as the rod bundles with spacer grid and mixing vanes. For example, the 2012 KAERI Matis experiment has tested the CFD predictions of the mixing flow in a complex geometry of subchannel behind a swirl-vane spacer grid. The Nek5000 LES submissions scored highly in the both blind benchmarks [63]. More recently, Busco *et al.* performed the validation of the wall resolved LES for the flow through a 5x5 fuel rod bundle with SGMV at a Reynolds number of 14,000 [64]. Excellent agreement was obtained between Nek5000 results and the particle image velocimetry (PIV) data. Built upon the great track record of Nek5000 in predicting flow physics in realistic reactor geometries, this study attempts to expand Nek5000 applicability to the MSR related phenomena.

4.1.1 Governing Equations and Turbulence Modeling

The incompressible formulation of Nek5000 is used in the current study which assumes a Newtonian fluid with constant properties. The corresponding continuity, momentum, and energy equations are listed below:

$$\frac{\partial u_i}{\partial x_i} = 0 \tag{4-1}$$

$$\frac{\partial u_i}{\partial t} + \frac{\partial}{\partial x_j}\left(u_i u_j\right) = -\frac{1}{\rho}\frac{\partial p}{\partial x_i} + \frac{\partial}{\partial x_j}\left[\nu\left(\frac{\partial u_i}{\partial x_j} + \frac{\partial u_j}{\partial x_i}\right)\right] \tag{4-2}$$

$$\frac{\partial T}{\partial t} + u_j\frac{\partial T}{\partial x_j} = \frac{\partial}{\partial x_j}\left(\frac{\nu}{Pr}\frac{\partial T}{\partial x_j}\right) + \frac{q}{\rho C_p} \tag{4-3}$$

where u is the velocity, p is the pressure, T is the temperature, ρ is the fluid density, ν stands for the kinematic viscosity, Pr is the Prandtl number, q is the heat generation in the fluid while C_p is the heat capacity.

Both LES and RANS approaches play unique roles here. The LES approach is utilized to produce high-fidelity reference data to reveal 3-D system responses in MSFR core, which uses the stabilizing filter of Fischer and Mullen [65]. The solution at each time step is explicitly filtered and the filtering operator F_α is defined as

$$F_\alpha = \alpha I_{\boldsymbol{N-1}} + (1-\alpha)\boldsymbol{I} \tag{4-4}$$

where $\boldsymbol{I}$ is the identity operator and $\boldsymbol{I_N}$ is the interpolation operator at the $N+1$ GLL nodes. This filter preserves the desirable spectral convergence of SEM as the mesh resolution increases. In addition, a characteristics based time-stepping [66] has been used in the LES runs to avoid the limitations imposed by the Courant-Friedrichs-Lewy (CFL) number due to the explicit treatment of the non-linear convection term.

Meanwhile, the $k-\omega$ model is among the most popular RANS turbulence models, which is known to offer better performance for boundary layer, free shear flows compared to other alternatives like $k-\varepsilon$ class of models. However, a main drawback associated is the wall boundary condition for ω. According to asymptotic estimates, the value of ω in the standard $k-\omega$ model becomes infinite at solid walls. The typical treatment is to specify the value of ω to some large value at grid points on the walls. Although this approach may increase stability, it causes the numerical solution to be sensitive to near-wall grid spacing [67]. The inability of this approach to provide a grid independent result aside, such treatment can be problematic in high-order approaches. For the spectral-element method used here, derivative operators are not local in character and assigning an arbitrarily large value at the wall can lead to numerical oscillations or divergence. In response, a novel regularized version of the standard $k-\omega$ turbulence model has been recently developed. Interested readers are referred to Tomboulides *et al.* [62] for more details of model implementation and validation concerning the regularized k − ω models in Nek5000. On the basis of regularized $k-\omega$ models, a variation, namely the $k-\tau$ model, is recently implemented with an emphasis on improved robustness and efficiency. It is to be further introduced in the following section.

4.1.2 Stability-enhanced Wall-resolved $k-\tau$ RANS model

The $k-\tau$ model was originally developed by Kalitzin *et al.* [60] as an alternative implementation of the $k-\omega$ model. The equations for k and τ are derived from the $k-\omega$ equations by using the definition $\tau = 1/\omega$:

$$\frac{\partial(\rho k)}{\partial t}+\nabla\cdot(\rho k\boldsymbol{v})=\nabla\cdot\left[\left(\mu+\frac{\mu_t}{\sigma_k}\right)\nabla k\right]+P-\rho\beta^*\frac{k}{\tau} \tag{4-5}$$

$$\frac{\partial(\rho \tau)}{\partial t}+\nabla\cdot(\rho \tau\boldsymbol{v})=\nabla\cdot\left[\left(\mu+\frac{\mu_t}{\sigma_\tau}\right)\nabla \tau\right]-\gamma\frac{\tau}{k}P+\rho\beta-2\frac{\mu}{\tau}(\nabla\tau\cdot\nabla\tau) \tag{4-6}$$

In contrast to the original form of the $k-\omega$ model, in which the ω equation contains terms that become singular close to wall boundaries, all terms in the right-hand side of the k and τ equations reach a finite limit at walls and do not need to be treated asymptotically; that is, they do not require regularization for numerical implementation. The eddy viscosity can be computed from the k and τ by

$$\mu_\tau=\rho k\tau \tag{4-7}$$

The Nek5000 version of $k-\tau$ has been benchmarked extensively across a variety of canonical cases including channel flow and the backward facing step, and it has been also applied to the fuel rod geometry recently. Interested readers are referred to Fang *et al*., [68] for more details regarding the $k-\tau$ application and validation in fuel rod bundles.

4.2 Problem Description

The specific reactor model considered herein is based upon the MSFR design created under the Euratom EVOL project [54]. The reference MSFR is a 3000 MW fast-spectrum reactor with three different circuits: the fuel circuit, the intermediate circuit, and the power conversion circuit. In the fuel circuit, there are 16 groups of pumps and heat exchangers around the core. Representative CFD models are established for the MSFR core region using the Nek5000. Leveraging the existing MSFR studies available in the literature, the "Geometry II" investigated by Rouch *et al.* [57] was selected as the reference geometry for our CFD simulations. The related investigations will first focus on the velocity distributions in the core cavity, which were used to demonstrate the applicability of NEAMS CFD code (*i.e.,* Nek5000) in MSFR related thermal-fluid problems. The next step is to include more physics in the MSFR core simulations, such as the heating and the tracking of delayed neutron precursors. Finally, the large scale full-core wall-resolved LES will be carried out to generate fundamental insights on the flow turbulence in core cavity given the access to necessary computational resources[1]. The related databases will be used to enhance the accuracy of RANS models, and also to calibrate the system analysis code or coarse-grid CFD programs directly used in MSFR design efforts.

A 2-D axisymmetric core model is first created for Nek5000 RANS simulations. The core has a height of 1.6 m along the centerline, and a height of 2.65 m in the peripheral region. The reactor radius ranges from 1.05 to 1.53 m. The peripheral wall is a curved surface, which resembles the shape of an hourglass. The 2-D geometric model and mesh are generated using the open source meshing software, GMSH [69]. The entire model consists of the core region and the inlet and outlet channels. Our scoping study shows that the curved wall and the bended inlet/outlet elbows are essential in producing a relatively uniform velocity distribution inside the core cavity. Moreover, the inlet channel is extruded accordingly to have a more developed inflow condition when the molten salt enters the core, while the extrusion of outlet helps prevent the backflow issue. A parabolic velocity profile is specified at the inlet face while the natural pressure boundary condition is given to the outlet face. The no-slip condition is applied to the reactor walls. A pure hexahedral mesh is generated with 3,700 elements (as shown in Figure 4-1). In addition, to facilitate the axisymmetric solver in Nek5000, the core centerline is rotated and aligned along the x-axis as shown in the Figure 4-1. The molten salt flow enters the core from the bottom channel (left) and exits from the top (right).

In addition to the 2-D RANS models, significant efforts have been invested in generating a more representative 3-D full core model to better study the related thermal-fluid phenomena in MSFR core cavity. The core height, diameter, inlet/outlet widths are kept the same as those used in the 2-D axisymmetric model. According to the proposed MSFR designs by the Euratom EVOL project, sixteen external loops are considered around the MSFR core. Note that the reactor components in the primary loop, such as the pumps and heat exchangers, are not modeled in this work. Future work may consider modeling these components via porous media models, especially for the heat exchanger region. Similar extrusion treatment is applied to the inlet and outlet faces to help the 3-D CFD model better converge. As mentioned earlier, the 3-D full core model will be simulated with the LES approach to allow a more accurate turbulence modeling compared to the 2-D RANS models. Since a full-fledged full core LES will require considerable

[1] A quick estimation shows that it requires over 3 million spectral elements, or 1 billion grid points to perform the wall-resolved LES of MSFR full core at Re = 250,000 (a quarter of the expected Reynolds number under the normal operating condition)

amount of computing power, a demonstrative full core LES case with the coarsened mesh and relatively low-polynomial order is conducted with the Nek5000, which proves the feasibility of a high-fidelity CFD model of the 3-D MSFR full-core. More details about the 3-D full core demonstration case can be found in the milestone report of Leite *et al.* [70].

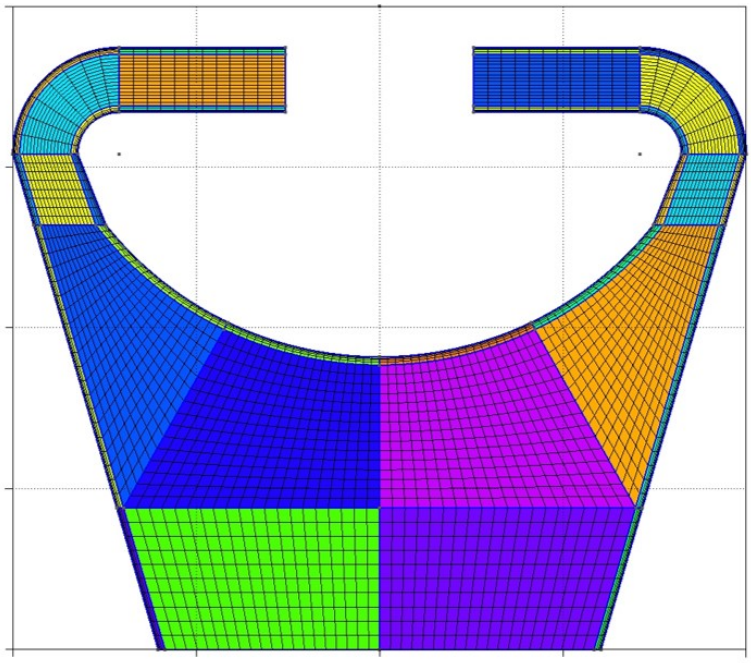

Figure 4-1: The mesh for the 2-D axisymmetric MSFR core model.

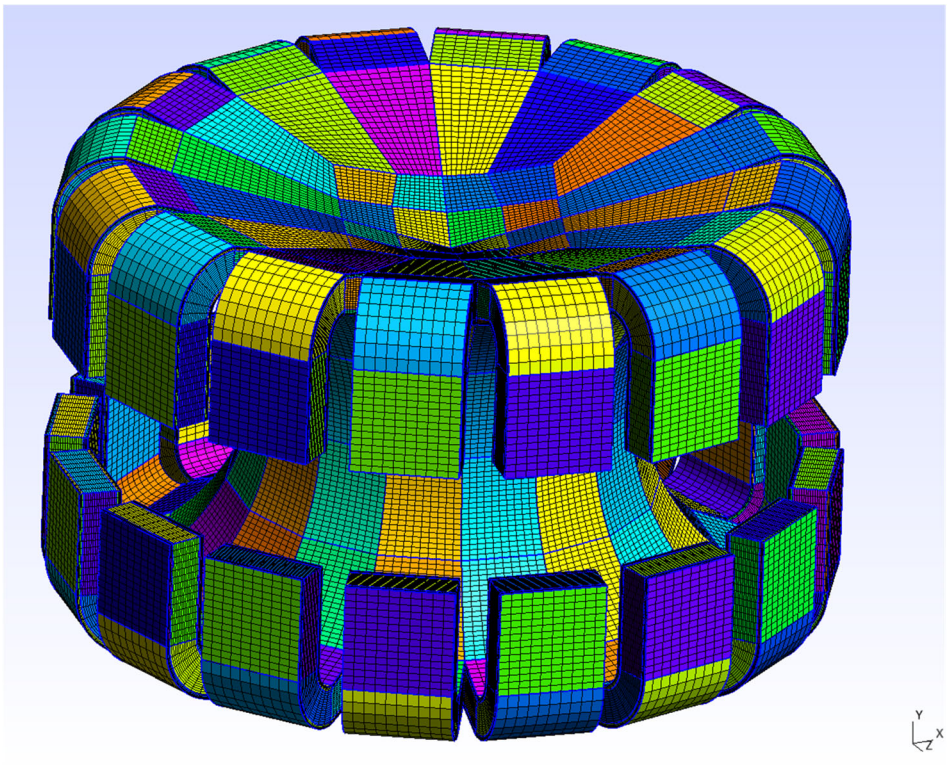

Figure 4-2: The mesh of the 3-D MSFR full core model.

4.3 Results and Discussion

The 2-D axisymmetric RANS case was simulated with a Reynolds number of ~40,000 at the minimum core diameter (at the central plane). After a quick transient stage, the simulations can reach the steady state. The corresponding steady-state solutions of non-dimensional velocity and turbulent kinetic energy (TKE) fields in the MSFR core are shown in Figure 4-3 and Figure 4-4. Higher velocity magnitudes are observed close to inlet and outlet elbows. Meanwhile, a large percentage of the bulk core sees a stable upward flow, which is desired for the MSFR system. As for the TKE field, the regions of large TKE value indicate strong local flow mixing. A velocity field with arrows is shown in Figure 4-5 to illustrate the velocity directions and magnitudes of specific locations inside the core. There is some minor recirculation predicted for this design as shown in the bottom left of the tank (in the blue region) in Figure 4-5, but there are significantly fewer compared to previous hypothetical fast MSR core designs that were previously modeled with Nek5000 [71]. An additional 2-D RANS simulation was carried out at a higher Reynolds number, 400,000, with the temperature solving. A prescribed non-dimensional heat source term is implemented as shown below.

$$q = 0.2 \cos\left(\frac{\pi}{2} \cdot \frac{x}{2.65}\right) \cos\left(\frac{\pi}{2} \cdot \frac{y}{1.935}\right) \tag{4-8}$$

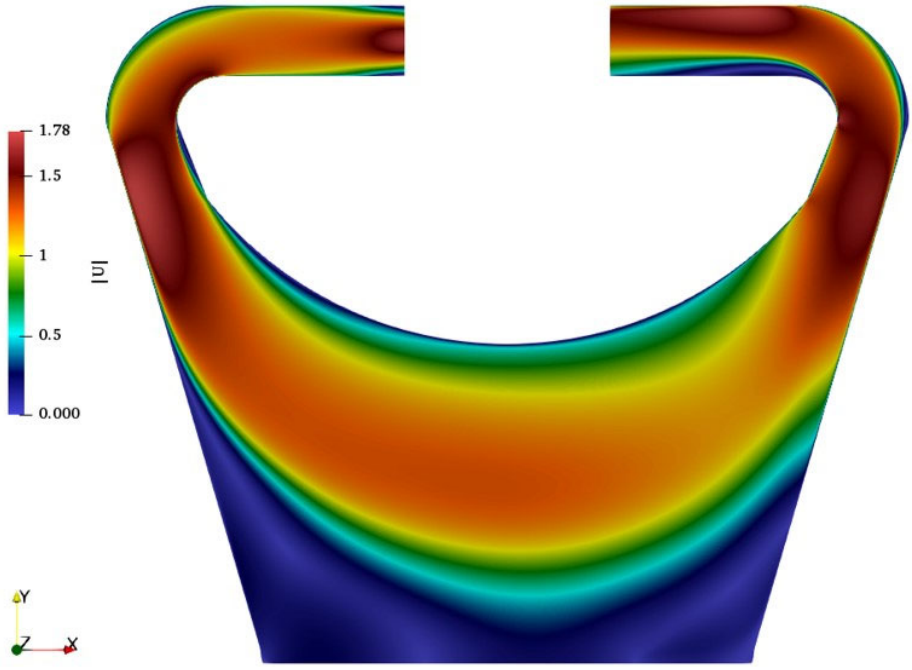

Figure 4-3: The steady-state velocity field from the 2-D MSFR RANS simulation at Re = 40,000.

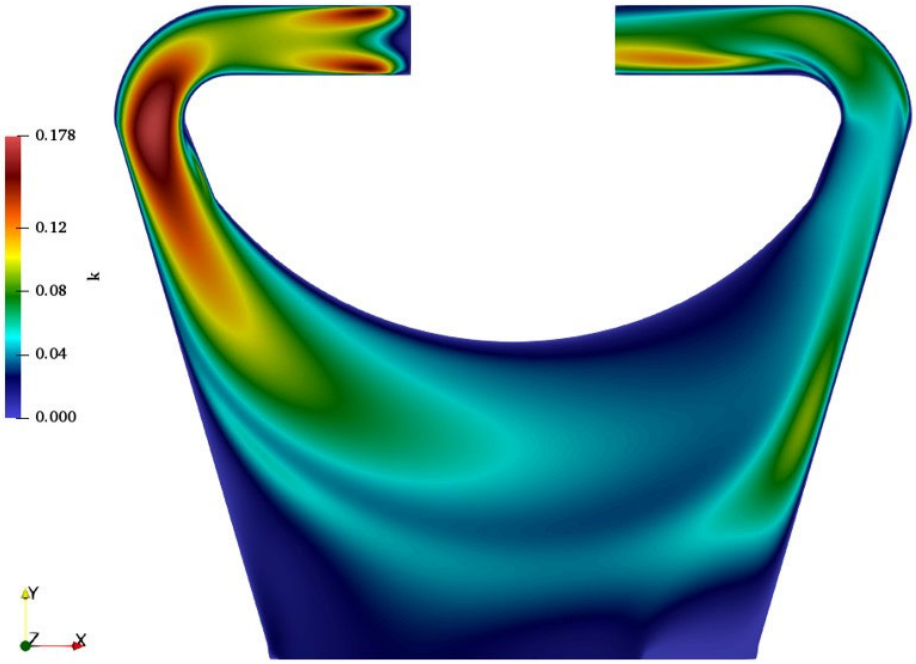

Figure 4-4: The steady-state TKE field from the 2-D MSFR RANS simulation at Re = 40,000.

Figure 4-5: The steady-state velocity field with arrows indicating local velocity directions.

The steady-state solution fields from the higher Reynolds number case are shown in Figure 4-6. Overall, the velocity distribution is very similar to that in Figure 4-3 with some difference in the maximum velocity value. On the other hand, the TKE field shows a subtle deviation from that in Figure 4-4. The high TKE region close to the inlet elbow remains prominent while the non-dimensional TKE becomes relatively lower in the rest of simulated domain. The non-dimensional temperature field at the steady state is illustrated in Figure 4-7 where the hot region

is observed to be around the core centerline. The average non-dimensional temperature at the outlet face is about 0.4. The tracking of DNPs would usually require the modeling of the entire primary loop that allows the long-half-life DNPs return to the core after circulating the primary loop, which will be investigated in the subsequent study.

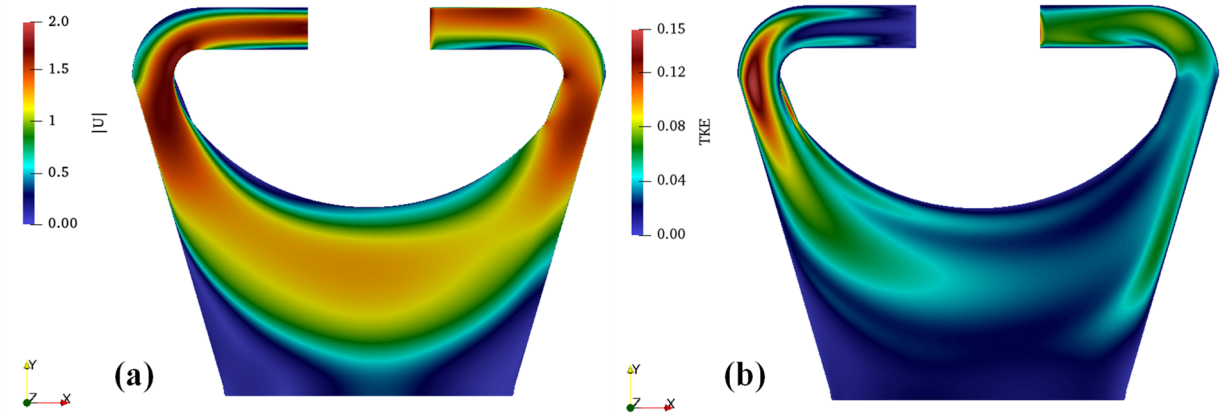

Figure 4-6: The steady-state solution fields of non-dimensional velocity (a) and turbulent kinetic energy (b) from the 2-D RANS simulation at Re = 400,000.

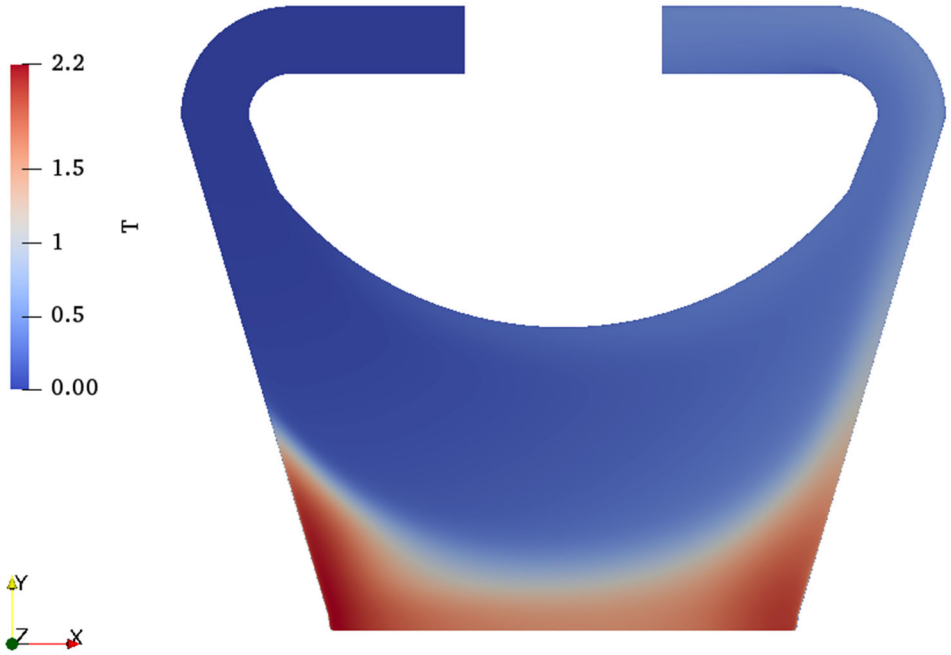

Figure 4-7: The steady-state non-dimensional temperature field from the 2-D RANS simulation at Re = 400,000.

4.4 Summary

To support the R&D efforts of the Molten Salt Fast Reactor (MSFR), a CFD model has been established for the MSFR core using the spectral element code, Nek5000. A $k-\tau$ model two-equation model was employed to model the turbulence. It has been demonstrated that the current simulation capability is capable to study the thermal-fluid phenomena inside the MSFR core.

Future studies will incorporate more relevant MSFR physics into the simulations, such as predicting the distributions of DNPs, calculating the hot spots inside the core. Besides the RANS and LES cases showcased in this work, future study will also consider expanding the high-fidelity Large Eddy Simulations (LES) for the MSFR system at affordable Reynolds numbers, and perform detailed comparisons between the high-fidelity LES results and the RANS solutions. The related numerical efforts will provide valuable insights to develop MSFR related thermal-hydraulics correlations, which will thus facilitate the MSFR design and optimization.

5 Systems Analysis

In FY21, the MSRE transient benchmark activity that started in FY19 was continued by performing additional validation calculations using the SAM [72] code based on MSRE experimental data collected from public literature and from ORNL documents [73]. These additional benchmark cases include three external reactivity insertion experiments of the MSRE at power levels of 1 MW, 5 MW, and 8 MW. The detailed description of the experimental sequence and the MSRE core geometry and material information can be found in Ref. [73]. The initial condition of the test is not clearly specified in Ref. [73], but the report suggests assuming that the fuel salt and coolant salt flows at full speed (1200 and 793 gpm). If this assumption were adopted, then the inlet/outlet temperatures at the core and primary heat exchanger (HX) cannot be fixed at the same time. For this study, the inlet temperature at the secondary side of the HX was assumed to be fixed at the design value of 819.3K. This assumption allows us to only model the primary loop of the MSRE.

5.1 Reactivity Insertion Test

For the reactivity insertion test, the SAM simulation consists of three steps:

1. In Step 1, a series of SAM calculations was performed to adjust the pump head in the primary loop and the heat transfer coefficient across the HX so that the designed operating condition (listed in Table 1) can be achieved, *i.e.*, the designed cold/hot temperatures of the primary and secondary loop can be reached at the designed operating power (10MW).
2. The power level was adjusted to be consistent with that in the experiments. The power was kept constant for a long period of time (1000 - 2000 seconds) until the steady state condition was achieved, *i.e.*, all parameters (density, temperature, *etc.*) in the system no longer change.
3. In the last step of the SAM calculation, an external reactivity was inserted at the beginning of the simulation, and power was allowed to change due to the external reactivity insertion and the reactivity feedback following the power increase.

Table 5-1: The design operating parameters for MSRE.

Parameter	Designed Value
Thermal Power [MW]	10
Core inlet temperature [K]	905.4
Core outlet temperature [K]	935.9
HX secondary inlet temperature [K]	819.3[1]
HX secondary outlet temperature [K]	852.6

1. This value is assumed to be fixed during the transient.

Several cases were modelled using SAM for the 5 MW reactivity insertion test using different approaches. The results are presented in Figure 5-1. The description of each case is summarized in Table 5-2. It should be noted that the moderator reactivity feedback coefficient was initially not an available input into SAM. In order to capture the feedback mechanism from the moderator (graphite in the MSRE), a request was sent to the SAM development team to add this capability in SAM, and it completed in time for this application.

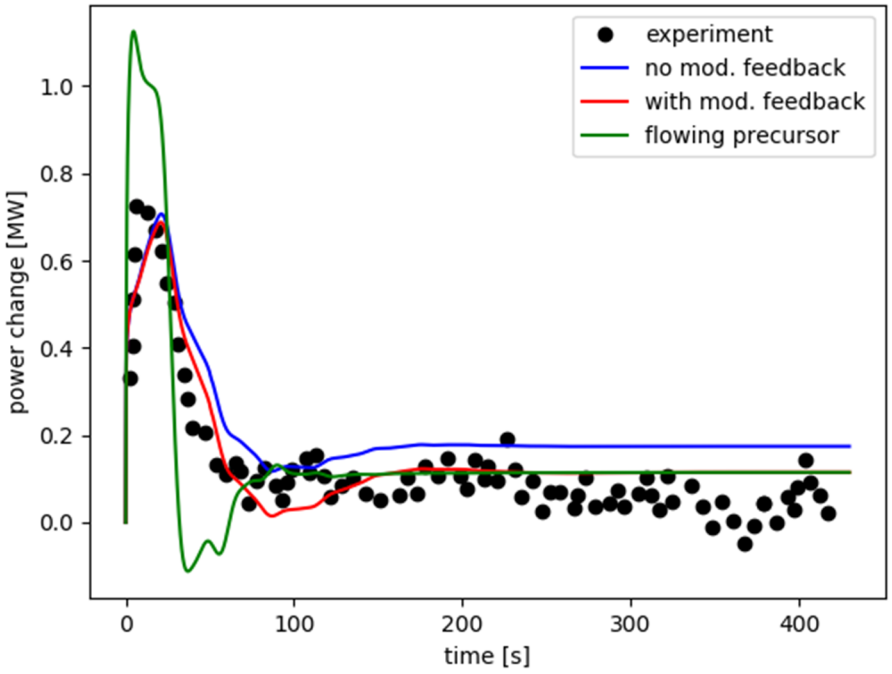

Figure 5-1: SAM simulation versus experimental data for the reactivity insertion transient at 5 MW.

Table 5-2: The parameters varied for each curve shown in Figure 5-1.

Legend label	Moderator feedback	Precursor drift
no mod. feedback	No	No
with mod. feedback	Yes	No
flowing precursor	Yes	Yes

We observed several things during the calculations and from results presented in Table 5-2 and Figure 5-1. These include:

1. The designed operating condition and the material properties specified in Ref. [73] are not agreeing with each other exactly. The relation that the designed core power (10MW) is equal to the designed mass flow rate (169.8 kg/s, calculated using 1200 gpm and 2.24 g/cm^3 average fuel density) multiplied by the temperature difference (30.6K) and the fuel salt specific heat (2385 J/kg-K) is only held true within some margin.
2. Moderator feedback has a non-negligible effect on the tail of the power evolution curve. Without the moderator feedback, the transient will reach an equilibrium state at a higher power level as the total negative reactivity is underestimated.
3. A large overestimation of the peak was observed when moving precursor modelling capability was enabled. Additional studies were performed to investigate this behavior, which is discussed in Section 5.2.

Additional parametric studies were performed to determine the impacts of having a finite insertion speed (instead of modeling an instant reactivity insertion in all the cases from Table 5-2). Different fuel reactivity feedback mechanisms were explored. In SAM, there are currently two fuel reactivity feedback mechanisms which are inputs: fuel density feedback and fuel

Doppler feedback. In the current SAM implementation, the fuel density feedback is linearly proportional to the temperature change, whereas the fuel Doppler feedback is inversely proportional to the fuel temperature. However, the fuel reactivity feedback coefficient provided from Ref. [74] is -6.13 pcm/F which combines both the Doppler and density feedback. Due to the lack of a neutronics model to separate the combined feedback coefficient, calculations were performed using this value for either the fuel density or Doppler reactivity coefficients separately and setting the other coefficient to zero. The results are presented in **Error! Not a valid bookmark self-reference.**, and **Error! Reference source not found.** lists the difference in each case.

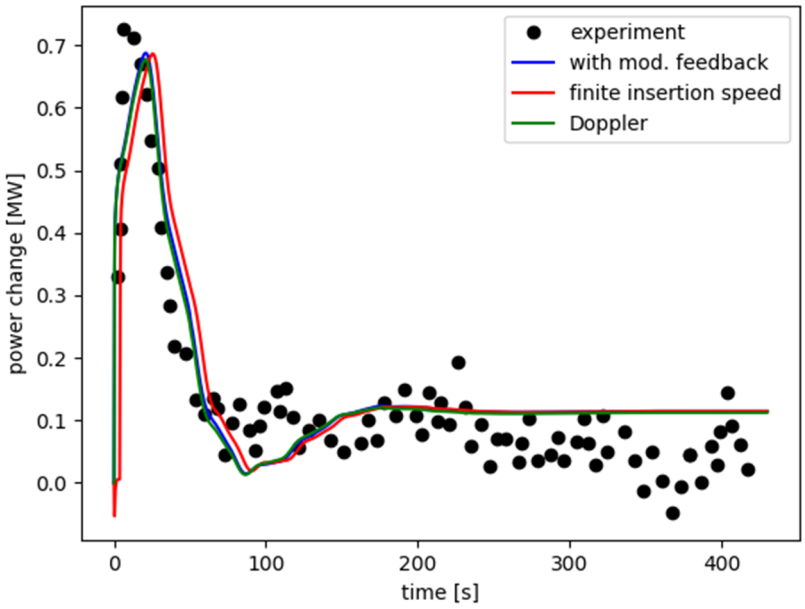

Figure 5-2: Additional parametric study results for the reactivity insertion transient at 5 MW.

Table 5-3: The parameters varied for each curve shown in Additional parametric studies were performed to determine the impacts of having a finite insertion speed (instead of modeling an instant reactivity insertion in all the cases from Table 5-2). Different fuel reactivity feedback mechanisms were explored. In SAM, there are currently two fuel reactivity feedback mechanisms which are inputs: fuel density feedback and fuel Doppler feedback. In the current SAM implementation, the fuel density feedback is linearly proportional to the temperature change, whereas the fuel Doppler feedback is inversely proportional to the fuel temperature. However, the fuel reactivity feedback coefficient provided from Ref. [74] is -6.13 pcm/F which combines both the Doppler and density feedback. Due to the lack of a neutronics model to separate the combined feedback coefficient, calculations were performed using this value for either the fuel density or Doppler reactivity coefficients separately and setting the other coefficient to zero. The results are presented in **Error! Not a valid bookmark self-reference.**, and **Error! Reference source not found.** lists the difference in each case.

.

Legend label	Moderator feedback	Precursor drift	Insertion speed	Fuel reactivity feedback

with mod. feedback	Yes	No	Infinite	Density feedback
finite insertion speed	Yes	No	~5 pcm/s	Density feedback
Doppler	Yes	No	Infinite	Doppler feedback

The difference between the Doppler and density reactivity feedback mechanism is very small due to the small temperature difference (1 – 2 K change). At such a small temperature change, the Doppler feedback is showing a linear relation with temperature change. With a finite insertion speed, the curve shifts to the right slightly.

Before moving to solve the overestimation problem observed for the 5 MW test with the precursor drift model, the SAM model (the reference case for the 5 MW test) was also used to simulate the 8 MW and 1 MW experiments. The results are presented in Figure 5-3 and Figure 5-4. We have found a possible error in the experiment specification, which lists the reactivities inserted for the 8 MW and 1 MW tests as 24.8 and 13.9 pcm, respectively. However, the reactivities inserted for the two tests may have been switched in the benchmark specification [75] based on the simulation results and literature review [76, 77]. The real reactivities inserted for the 8 MW and 1 MW tests should be 13.9 and 24.8 pcm, respectively. After switching, the SAM simulations without drift show very good agreement with the experimental measurement for the 8 MW test and closer but not good agreement for the 1 MW test. Note that for all 3 cases, when drift is included, there is an overshoot in the power change near the beginning of the simulation compared to measurements. In the subsequent studies, we focused on solving the overestimation problem for the 5 MW first, as we expected that solving this problem would also benefit solving the overshooting problem for the 1 MW and 8 MW cases.

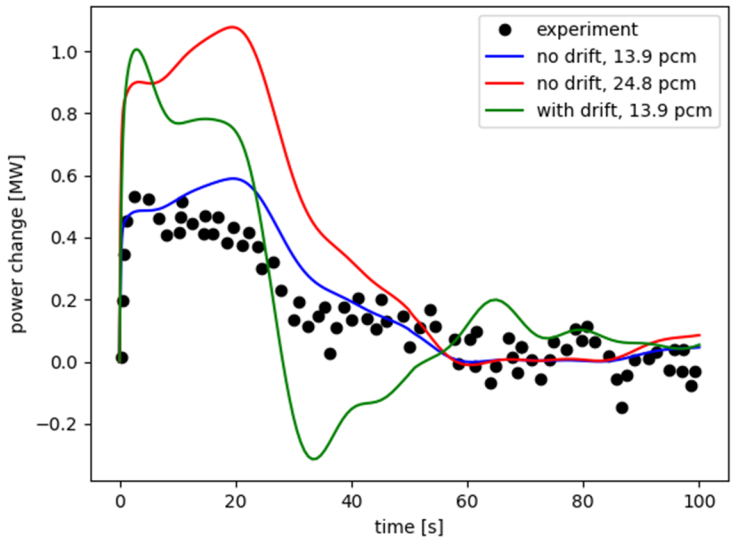

Figure 5-3: SAM simulation versus experimental data for the reactivity insertion transient at 8 MW (correct reactivity insertion is presumed to be 13.9 pcm).

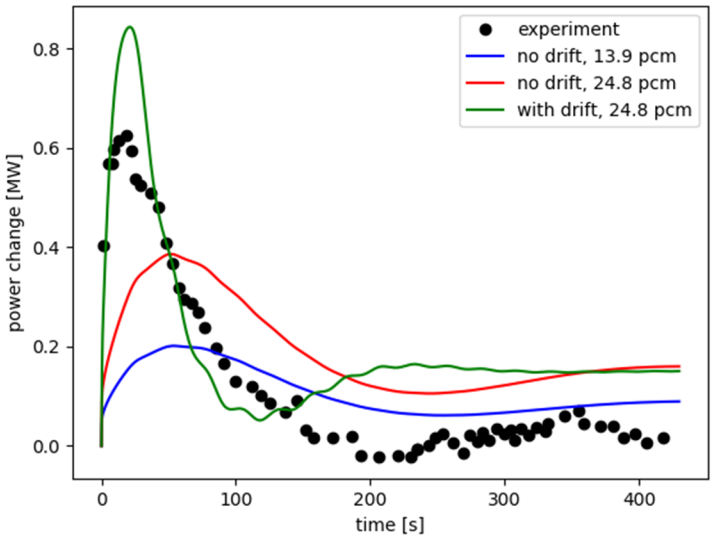

Figure 5-4: SAM simulation versus experimental data for the reactivity insertion transient at 1 MW (correct reactivity insertion is presumed to be 24.8 pcm).

5.2 Sensitivity Study of the 5 MW Test

As discussed in the previous subsection, overestimation of the peak was observed for both the 1 MW and 5 MW cases when the precursor drift model was enabled in the SAM calculation. Different approaches were tested to resolve this discrepancy, focusing on the 5 MW test as the reference case. These include:

1. use of different axial power shape,
2. use of finite reactivity insertion speed,
3. use of more precursor groups,
4. use of different power models for the fuel and moderator,
5. use of two core channels,
6. use of non-uniform axial coolant density reactivity feedback coefficient,
7. addition of precursor source term in the upper and lower plenum.

The results for the first three approaches show minimal changes. Using sine-shaped and uniform axial power does not change the results as presented in Figure 5-5. Figure 5-6 shows that using finite reactivity insertion only shifts the curve to the right slightly compared to that for the model without precursor drift. Using 8 precursor groups also does not change the result significantly as presented in Figure 5-7.

The fourth approach assigned different power splits in the fuel salt and the moderator. The particles (fission products, gamma, neutron, *etc.*) created during the nuclear fission deposit their energy in both fuel and moderator. However, specifying the fraction of total power deposited in the moderator is not allowed in SAM. This means that the current version of SAM does not enable the moderator power to change in response to reactivity feedback since the moderator heat deposition cannot be related to the total reactor power. For testing purposes, a constant value (7% of the total power) was assigned for the power generated in the moderator. The current version of SAM does not enable the moderator power to change in response to reactivity

feedback. In any case, it was assumed that this approximation (constant power in moderator) would not affect the results of the reactivity insertion tests due to the small power change.

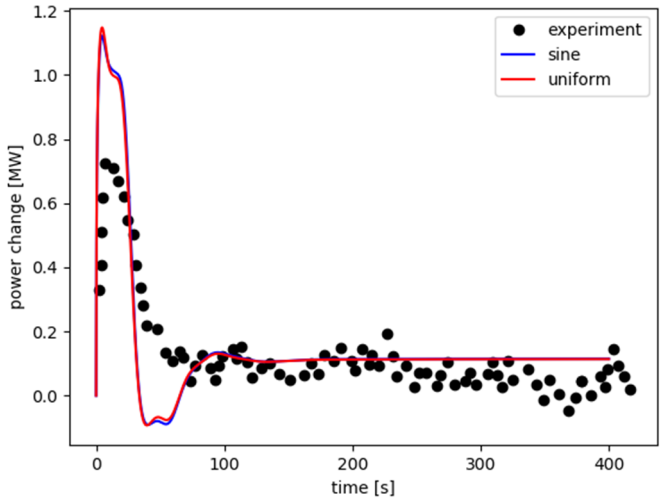

Figure 5-5: Effect of power axial profile on the reactivity insertion test result.

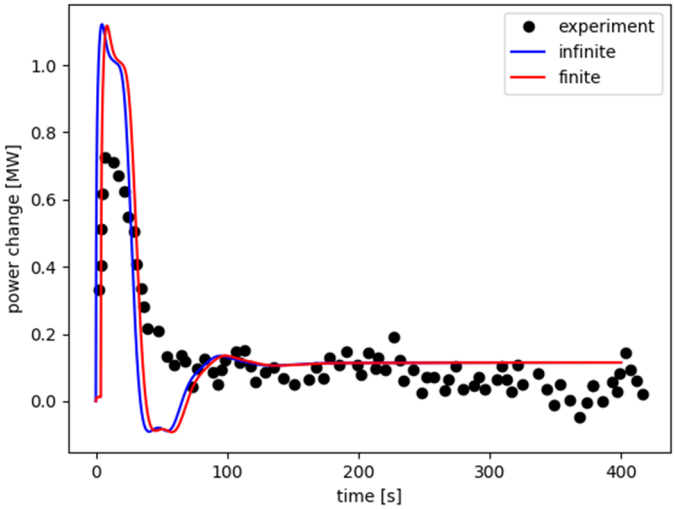

Figure 5-6: Effect of the reactivity insertion speed on the reactivity insertion test result.

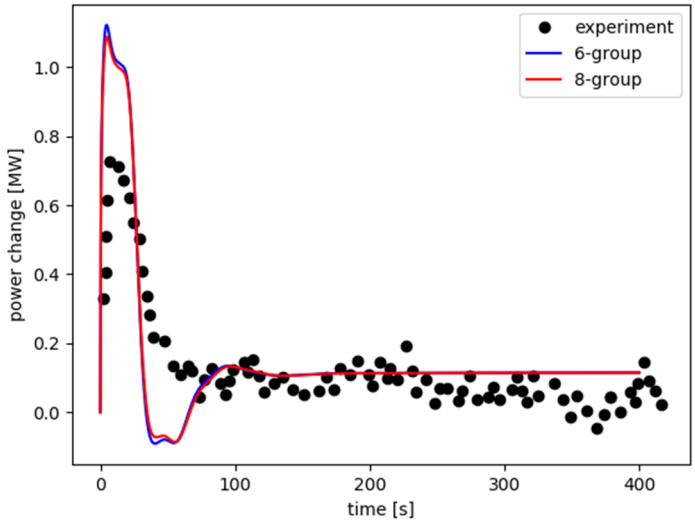

Figure 5-7: Effect of number of precursor groups on the reactivity insertion test result.

The percent of power generated in the fuel salt was adjusted to 93% of the total power, as represented by the red curve in Figure 5-8. The default setting is 100% of the power is generated in the fuel salt, as represented by the blue curve. Figure 5-8 shows that the transient is very sensitive to this variation, since decreasing the total power generated in the fuel salt significantly underestimates the precursors produced in the fuel channel. In other words, there is a mismatch between the reactor total power and the power produced in the fuel where the delayed neutron precursor is produced. If these power splits were reflective of the actual conditions, then 93% of the power would have been generated in the fuel salt, but 100% of the delayed neutron precursors would have been generated in the fuel. However, SAM models this delayed neutron precursor being reduced as well and normalized to the wrong total power. Thus, the power fraction in the fuel and the precursor fraction in the fuel need to be separated in the future development of SAM. This separation is important for the SAM code to model the reactor kinetics and the temperature distribution correctly for MSRs with flowing fuel salt.

Another approach was explored based on the observation discussed above. In this approach, the total reactor power was reduced to 93% of the reference value (5 MW). The power in the fuel was set to 100% of the total power. A constant power (7% of 5 MW) was assigned to the moderator. In this case, the effect on the SAM result is negligible. This is illustrated by the blue and green curves in Figure 5-8. These preliminary assessments indicate that the SAM-calculated peak in the power change that occurs in the first few seconds is strongly dependent on the power fraction and precursor fraction terms, and further testing of it is recommended once these two terms are separated in SAM.

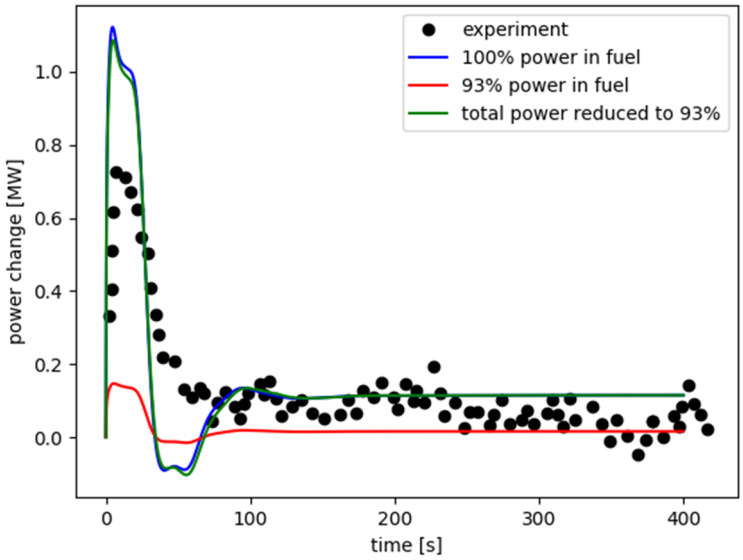

Figure 5-8: Effect of reducing the total power on the SAM result.

Using multiple core channels also did not solve the problem as shown in Figure 5-9. The MSRE core is divided into two channels with equal flow area. Two cases were examined with different power distribution. The power fraction in the inner channel is 0.6 in one case and 0.7 in the other. However, the effects on the SAM result in both cases were small.

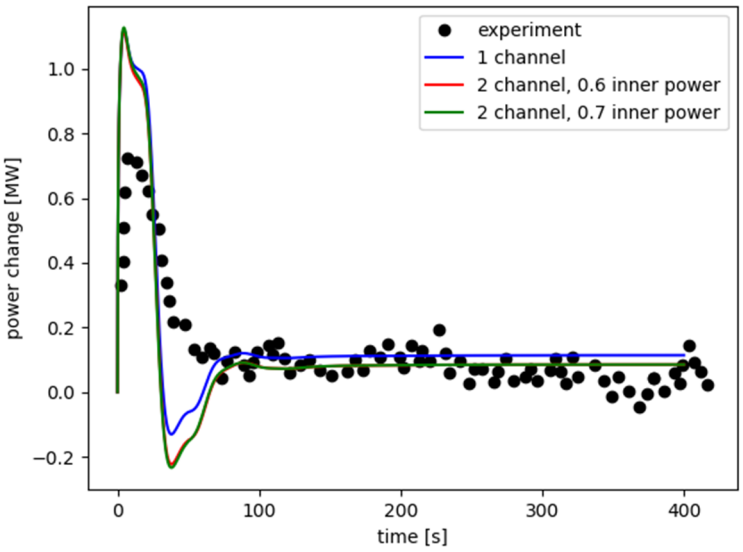

Figure 5-9: Effect of using multiple channels on the SAM results

We also tried to include the DNPs generated in the upper and lower plenum. Small modifications of the SAM point kinetics model were made to allow more flexibility in configuring the precursor source and point kinetic equation. More details of the modifications are described in the next section (Section 5.3). Several cases were investigated using the modified SAM code. Their main differences are listed in Table 5-4. The "source channel" includes the channels with delayed neutron precursor source. The "flowing-in" and "flowing-out" channels are the channels included in the initialization process as represented by the $\dot{c}_{in,i}(0) - \dot{c}_{out,i}(0)$ term in Equation 5-1. The "integrate" channels are those included in the integration of the precursor concentrations

($\lambda_i C_i$ term in Equation 5-1). The results for all the cases are compared in Figure 5-10. Case 4 agrees very well with the experimental data and is highlighted in Figure 5-11. This suggests including precursor in the upper and lower plenum is important for the reactivity insertion tests.

$$\frac{\mathrm{dn}}{\mathrm{dt}} = \frac{\rho - \beta - \sum_i \left(\dot{c}_{in,i}(0) - \dot{c}_{out,i}(0)\right)\Lambda}{\Lambda} n + \sum_i \lambda_i C_i, \tag{5-1}$$

Table 5-4: Summary of the different cases investigated for adding precursor source in the upper and lower plenum.

Case #	Channels			
	Source	Flowing-in	Flowing-out	Integrate
0*	Core	Core	Core	Core
1	Core, Upper plenum	Core	Core	Core
2	Core, Upper plenum	Core	Upper plenum	Core, Upper plenum
3	Core, Upper plenum, Lower plenum	Core	Core	Core
4	Core, Upper plenum, Lower plenum	Lower plenum	Upper plenum	Core, Upper plenum, Lower plenum

* This is the original case.

The approach used for the 5 MW test was adopted for the 1 MW and 8 MW tests. The results are presented in Figure 5-12 and Figure 5-13 for the 8 MW and 1 MW tests, respectively. Significant improvement was also observed for the 8 MW test, but not for the 1 MW test. We suspect that the boundary condition assumed (constant inlet temperature of the secondary side of the heat exchanger) may not have been true for the 1 MW case due to the low power level. Further investigation will be needed in the future.

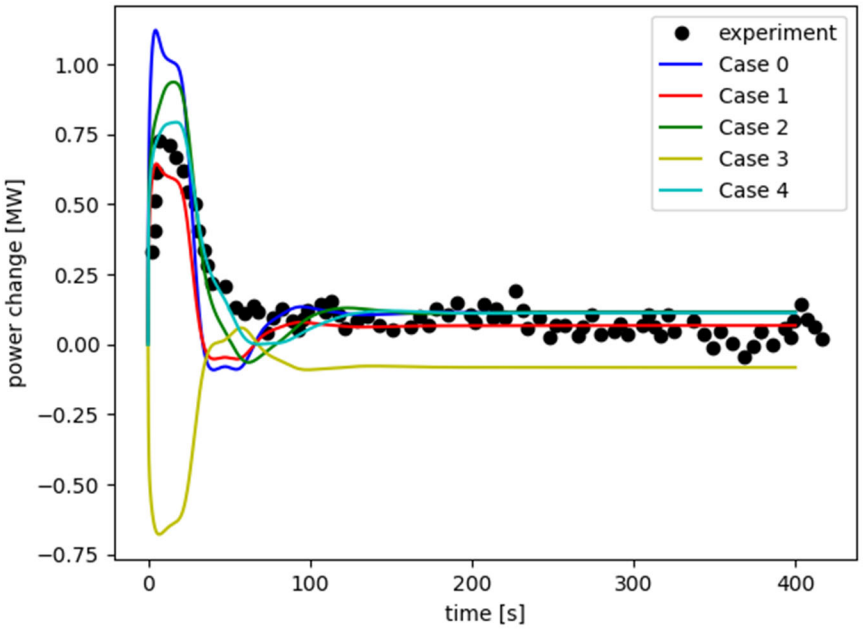

Figure 5-10: Comparison of the SAM results and the experimental data for the 5 MW reactivity insertion test.

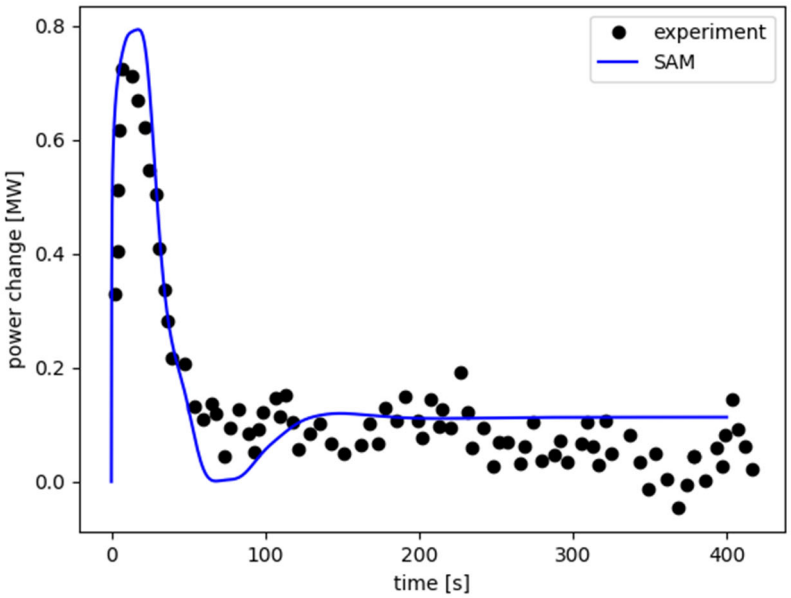

Figure 5-11: Comparison of Case 4 result and the experimental data.

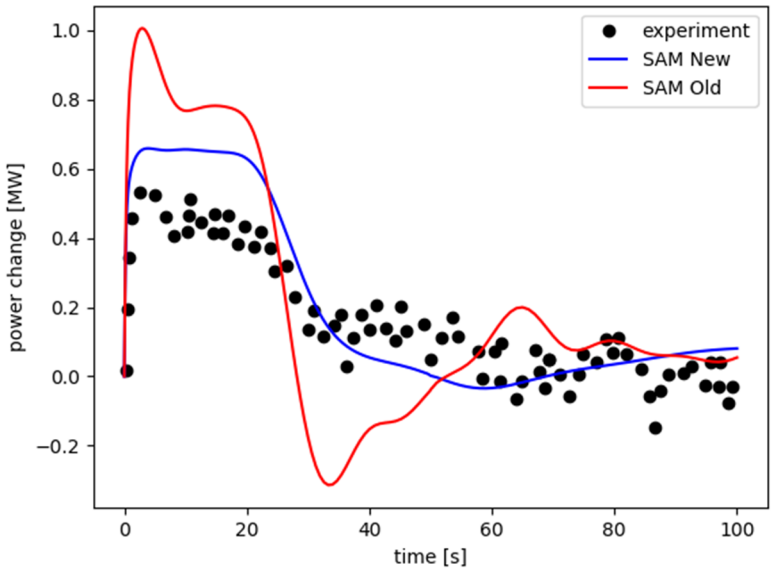

Figure 5-12: Comparison of the SAM results and the experimental data for the 8 MW reactivity insertion test.

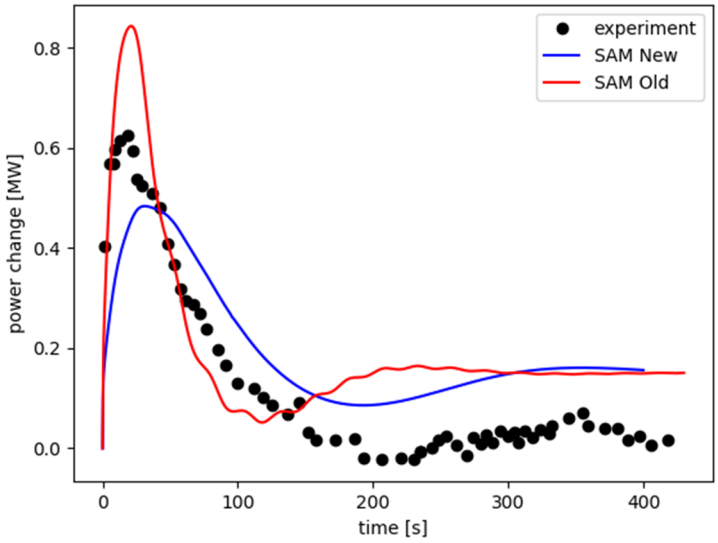

Figure 5-13: Comparison of the SAM results and the experimental data for the 1 MW reactivity insertion test.

5.3 Modification of SAM

The following modifications of SAM were implemented and used in the generation of the results in Table 5-4 but not for results before it. The current SAM point kinetic equation is implemented as Equation 5-1 combined with Equation 5-2 and 5-3. c_i is the number of delayed neutron precursors per kg of fuel, and C_i is the total population of the precursors in the channels with precursor source. Thus, Equation 5-2 is essentially the integration of Equation 5-3 in all channels with precursor source. Solving Equation 5-2 can be completely avoided by integrating c_i along

the channels with precursor source as depicted in Equation 5-4. This modification has little impact on the results for the reactivity insertion test as illustrated in Figure 5-14.

$$\frac{\mathrm{dC_i}}{\mathrm{dt}} = \frac{\beta_i}{\Lambda} n - \lambda_i C_i + \left(\dot{c}_{in,i} - \dot{c}_{out,i}\right). \tag{5-2}$$

$$\frac{\partial \rho c_i}{\partial t} + \frac{u \partial \rho c_i}{\partial x} = \frac{\beta_i}{\Lambda} n - \lambda_i \rho c_i \tag{5-3}$$

$$C_i(t) = \sum_{j(\#\ channels)} \int \rho(x,t) c_{i,j}(x,t) dx \tag{5-4}$$

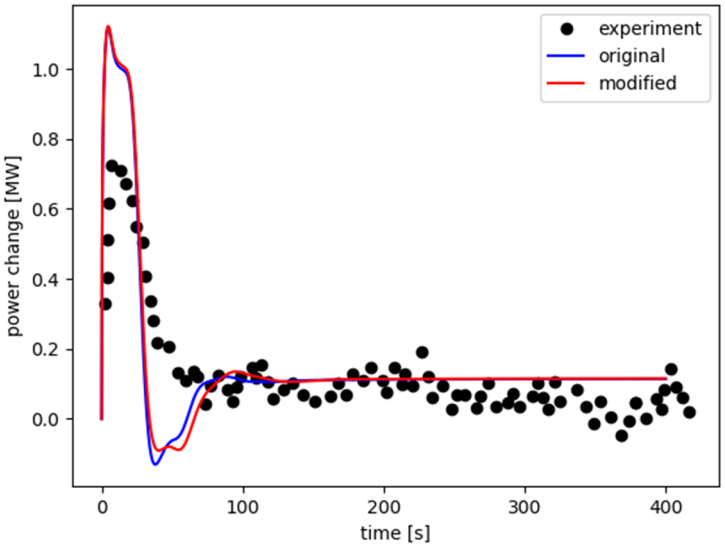

Figure 5-14: Comparison of the original and modified SAM results of Case 1 in Table 5-4

The SAM point kinetic equation implementation was further modified to separate the precursor source, flowing-in, flowing-out, and integration channels. This allows more flexibility of using the point kinetic model in SAM. It also removes redundant postprocessors for the flowing-in and flowing-out precursor terms ($\dot{c}_{in,i}(0) - \dot{c}_{out,i}(0)$ term in Equation 5-1).

In addition, the following modifications are suggested for SAM:

1. Adding the capability in SAM to allow the moderator power change proportionally with the reactor power.
2. Separate the power fraction and the delayed neutron precursor fraction as the two parameters can have different value in reality.

6 Summary

The main goal of this work was to identify the modeling and simulation functional requirements for designing, licensing, and operating MSRs and apply those capabilities already developed in NEAMS tools to example problems of interest. The four main parts of this report each focuses on a specific area of simulation physics as it relates to MSR phenomena: fuel evolution, chemistry, CFD, and systems analysis.

In terms of fuel evolution, which includes depletion, decay, on-line separations, and transmutation, the current state of computational capabilities for modeling this behavior in liquid-fueled molten salt reactor is discussed. Some of the functional requirements to accomplish the various applications of MSR fuel depletion modeling are highlighted, followed by a summary of recent approaches and code development activities.

The chemistry functional requirements were discussed in the context of several applications of high importance for MSRs, such as corrosion, salt chemistry, and species transport. Each of these types of chemistry modeling have considerable impact on various aspects of reactor applications, including informing on reactor designs, improving operational efficiencies, analyzing safety and reactivity concerns, and estimating the mechanistic source term of the reactor. A brief overview is also provided on code development activities ongoing under NEAMS relevant to chemistry modeling of MSRs.

In terms of CFD applications, the state-of-the-art spectral element code, Nek5000 was used to model the fluid dynamics within a full core of the Molten Salt Fast Reactor (MSFR) concept designed as part of the Euratom EVOL project. This concept was selected as the challenge problem because of its similar features to several U.S. industry concepts. The goal was to model some of the fast MSR design challenges, including potential large internal re-circulation, the need of accurate tracking of delayed neutron precursors (DNP), and the lack of relevant thermal-hydraulics models/correlations, *etc.* Therefore, a series of CFD models were created for the MSFR core cavity using a $k - \tau$ model two-equation model for the turbulence. These first full core results demonstrated that any potential recirculation zones could be properly identified with the current NEAMS CFD capabilities. The development of these models will also set the stage for future testing of Nek5000's functionalities to model other MSR thermal-fluid phenomena.

Lastly, the validation of SAM against experimental data from the Molten Salt Reactor Experiment, which started in FY19, continues with the inclusion of modeling the reactivity insertion tests. This involved using SAM and its point kinetics model for flowing fuel salt to recreate the time dependent power changes and response after positive reactivity insertions at the 1, 5, and 8 MWt power levels. Through these exercises, several code modifications were suggested to the SAM development team and accommodated to enable closer agreement with solid technical and physical justifications. These include adding a moderator reactivity feedback coefficient as an available input and modifying the solution approach for the point kinetics model. Additional SAM development suggestions for flowing fuel MSRs include adding the capability to allow the moderator power change proportionally with the reactor power and enabling specification of the power and DNP distributions separately.

7 Acknowledgements

This research was supported by the Nuclear Energy Advanced Modeling and Simulation (NEAMS) program of the Department of Energy, Office of Nuclear Energy (DOE-NE). The authors would like to thank Thanh Hua from ANL and Dane De Wet and Ben Betzler from ORNL with whom we worked closely on the NEAMS MSR Application Drivers activity through frequent meetings, discussions, and correspondences.

8 References

[1] S. Shahbazi *et al.*, "Survey and Assessment of Computational Capabilities for Advanced (non-LWR) Reactor Mechanistic Source Term Analysis," Argonne National Laboratory and Sandia National Laboratories, ANL/NSE-20/39, SAND2021-3250R, September 2020.

[2] A. Rykhlevskii, "Fuel processing simulation tool for liquid-fueled nuclear reactors," PhD Thesis, University of Illinois, Urbana-Champaign, 2020.

[3] A. Worrall, J. W. Bae, B. R. Betzler, M. S. Greenwood, and L. G. Worrall, "Molten Salt Reactor Safeguards: The Necessity of Advanced Modeling and Simulation to Inform on Fundamental Signatures," in *Proceedings from 60th INMM Meeting*, 2019.

[4] X. Doligez, D. Heuer, E. Merle-Lucotte, M. Allibert, and V. Ghetta, "Coupled study of the Molten Salt Fast Reactor core physics and its associated reprocessing unit," *Annals of Nuclear Energy,* vol. 64, pp. 430-440, 2014.

[5] A. J. H. Lee, "Neutronics and thermal-hydraulics analysis of transatomic power molten salt reactor (TAP MSR) core under load following operations," M.S. Thesis, University of Illinois, Urbana-Champaign, 2020.

[6] L. R. Cornejo, B. R. Betzler, K. Myhre, and J. McFarlane, "Modeling molybdeneum-99 production in molten salt reactors," *Nuclear Engineering and Design,* vol. 379, 2021.

[7] C. Johnson, J. L. Slack, M. K. Sharma, C. K. Simpson, and J. L. Burnett, "Modeling of fission and activation products in molten salt reactors and their potential impact on the radionuclide monitoring stations of the International Monitoring System," *J Environ Radioact,* vol. 234, p. 106625, May 3 2021.

[8] B. Betzler, "Liquid-fueled Molten Salt Reactor Depletion Modeling," presented at the ANS Annual Meeting, Virtual, June, 2021.

[9] B. R. Betzler, J. J. Powers, and A. Worrall, "Molten salt reactor neutronics and fuel cycle modeling and simulation with SCALE," *Annals of Nuclear Energy,* vol. 101, pp. 489-503, 2017.

[10] S. E. Creasman, "Methodology for Source Term Analysis of a Molten Salt Reactor," M.S. Thesis, University of Tennessee, Knoxville, 2020.

[11] B. R. Betzler, K. B. Bekar, W. A. Wieselquist, S. W. Hart, and S. G. Stimpson, "Molten Salt Reactor Fuel Depletion Tools in SCALE," presented at the Global 2019, Seattle, WA, September 22-27, 2019.

[12] M. Aufiero, "Development of Advanced Simulation Tools for Circulating-Fuel Reactors," PhD Thesis, Energy and Nuclear Science and Technology, Politecnico Di Milano, 2014.

[13] O. Ashraf, A. Rykhlevskii, G. V. Tikhomirov, and K. D. Huff, "Whole core analysis of the single-fluid double-zone thorium molten salt reactor (SD-TMSR)," *Annals of Nuclear Energy,* vol. 137, 2020.

[14] A. M. Wheeler, V. Singh, L. F. Miller, and O. Chvála, "Initial calculations for source term of Molten Salt Reactors," *Progress in Nuclear Energy,* vol. 132, 2021.

[15] A. G. Nelson, "User Guide to the Advanced Dimensional Depletion for Engineering of Reactors (ADDER) Software," Argonne National Laboratory, ANL/RTR/TM-21/8, April 2021.

[16] A. G. Nelson, J. A. Stillman, F. Heidet, and E. H. Wilson, "The ADDER Software for Reactor Depletion and Fuel Management Analysis," presented at the 2020 American Nuclear Society Winter Meeting, Virtual, November, 2020.

[17] A. G. Nelson, G. J. Y. Chee, and M. G. Jarrett, "Molten Salt Reactor Depletion Techniques in the ADDER Reactor Depletion and Fuel Management Analysis Code," presented at the ANS M&C 2021 - The International Conference on Mathematics and Computational Methods Applied to Nuclear Science and Engineering (accepted), Raleigh, North Carolina, October 3-7, 2021.

[18] R. Z. Taylor, "Libowski: A Numerical Framework for Solving Depletion and Mass Transport in Molten Salt Reactors," PhD Thesis, Department of Nuclear Engineering, University of Tennessee, Knoxville, 2021.

[19] C. Lee *et al.*, "Griffin Software Development Plan," Argonne National Laboratory, Idaho National Laboratory, ANL/NSE-21/23, INL/EXT-21-63185, June 2021.
[20] S. Shahbazi and D. Grabaskas, "Functional Requirements for the Modeling and Simulation of Advanced (Non-LWR) Reactor Mechanistic Source Term," Argonne National Laboratory, ANL/NSE-20/17, June 2020.
[21] S. Shahbazi and D. Grabaskas, "A Pathway for the Development of Advanced Reactor Mechanistic Source Term Modeling and Simulation Capabilities," Argonne National Laboratory, ANL/NSE-21/21, May 2021.
[22] A. Graham, R. R. Pillai, B. S. Collins, and J. W. McMurray, "Engineering scale molten salt corrosion and chemistry code development," ORNL/SPR-2020/1582, July 2020.
[23] R. A. Lefebvre, B. R. Langley, P. Miller, M. Delchini, and M. L. Baird, "NEAMS Workbench Status and Capabilities," Oak Ridge National Laboratory, ORNL/TM-2020/1731, September 2020.
[24] J. D. Stempien, "Tritium transport, corrosion, and Fuel performance modeling in the Fluoride Salt-Cooled High-Temperature Reactor," PhD Thesis, Nuclear Science & Engineering, Massachusetts Institute of Technology, 2015.
[25] N. Hoyt and H. Yuan, "Thermogalvanic Modeling Capabilities to Support Engineering-Scale Corrosion Simulations," Argonne National Laboratory, ANL/CFCT-20/36, September 2020.
[26] T. M. Besmann *et al.*, "Corrosion System-Focused Expansion and Application of the Thermochemical Database for Molten Salt Reactors- MSTDB-TC," presented at the ANS Annual Meeting, Virtual, June, 2021.
[27] S. Shahbazi, S. Thomas, A. Merwin, Q. Zhou, and M. Bucknor, "Thermochemical Modeling in Molten Fluoride Salts for Radionuclide Speciation," Argonne National Laboratory, ANL/KP-21/1, KP-RPT-000139, February 2021.
[28] H. E. McCoy and B. McNabb, "Intergranular Cracking of INOR-8 in the MSRE," Oak Ridge National Laboratory, ORNL-4829, November 1972.
[29] W. Zhou *et al.*, "Proton irradiation-decelerated intergranular corrosion of Ni-Cr alloys in molten salt," *Nat Commun,* vol. 11, no. 1, p. 3430, Jul 9 2020.
[30] A. Abou-Jaoude, S. A. Walker, S. Bhaskar, and W. Ji, "Feasibility Assessment of a Natural-Circulation Salt Irradiation Loop in the Advanced Test Reactor," *Nuclear Technology,* pp. 1-21, 2021.
[31] A. D. Pelton, P. Chartrand, and G. Eriksson, "The modified quasi-chemical model: Part IV. Two-sublattice quadruplet approximation," *Metallurgical and Materials Transactions A,* vol. 32A, pp. 1409-1416, 2001.
[32] J. W. McMurray, T. M. Besmann, J. Ard, S. Utlak, and R. A. Lefebvre, "Status of the molten salt thermodynamic database, MSTDB," Oak Ridge National Laboratory, ORNL/SPR-2019/1208, August 2019.
[33] J. W. McMurray *et al.*, "Roadmap for thermal property measurements of Molten Salt Reactor systems," ORNL/SPR-2020/1865, March 2021.
[34] M. H. A. Piro, S. Simunovic, T. M. Besmann, B. J. Lewis, and W. T. Thompson, "The thermochemistry library Thermochimica," *Computational Materials Science,* vol. 67, pp. 266-272, 2013.
[35] M. Poschmann, B. W. N. Fitzpatrick, S. Simunovic, and M. H. A. Piro, "Recent Development of Thermochimica for Simulations of Nuclear Materials," in *TMS 2020 149th Annual Meeting & Exhibition Supplemental Proceedings*, 2020, pp. 1003-1012.
[36] P. Bajpai, M. Poschmann, D. Andrš, C. Bhave, M. Tonks, and M. Piro, "Development of a New Thermochemistry Solver for Multiphysics Simulations of Nuclear Materials," in *TMS 2020 149th Annual Meeting & Exhibition Supplemental Proceedings*(The Minerals, Metals & Materials Series, 2020, pp. 1013-1025.
[37] P. J. Vicente-Valdez, B. R. Betzler, W. A. Wieselquist, and M. Fratoni, "Modeling Molten Salt Reactor Fission Product Removal with SCALE," Oak Ridge National Laboratory, ORNL/TM-2019/1418, February 2020.
[38] Z. Taylor, "Implementation of Multi-phase Species Transport into VERA-CS for Molten Salt Reactor Analysis," M.S. Thesis, University of Tennessee, Knoxville, 2019.

[39] S. A. Walker and W. Ji, "Species transport analysis of noble metal fission product transport, deposition, and extraction in the molten salt reactor experiment," *Annals of Nuclear Energy,* vol. 158, 2021.
[40] R. J. Kedl and A. Houtzeel, "Development of a Model for Computing 135Xe Migration in the MSRE," Oak Ridge National Laboratory, ORNL-4069, June 1967.
[41] T. Price, O. Chvala, and G. Bereznai, "A dynamic model of xenon behavior in the Molten Salt Reactor Experiment," *Annals of Nuclear Energy,* vol. 144, 2020.
[42] T. J. Price, O. Chvala, and Z. Taylor, "Xenon in molten salt reactors: The effects of solubility, circulating particulate, ionization, and the sensitivity of the circulating void fraction," *Nuclear Engineering and Technology,* 2020.
[43] T. Fei, T. Hua, B. Feng, F. Heidet, and R. Hu, "MSRE Transient Benchmarks using SAM," presented at the PHYSOR 2020: Transition to a Scalable Nuclear Future, Cambridge, U.K., March 29 - April 2, 2020.
[44] S. A. Walker, Z. Taylor, R. Salko, B. Collins, and W. Ji, "Noble Metal Mass Transport Model for Molten Salt Reactor Analysis in VERA-CS," presented at the M&C 2019, Portland, OR, August 25-29, 2019.
[45] A. Graham, B. Collins, R. Salko, Z. Taylor, and C. Gentry, "Development of Molten Salt Reactor Modeling and Simulation Capabilities in VERA," presented at the Global/Top Fuel 2019, Seattle, WA, September 22-27, 2019.
[46] R. Salko, A. Graham, R. A. Lefebvre, and B. Langley, "Demonstration of MSR Salt Property Database Operation with a Reactor Analysis Tool," Oak Ridge National Laboratory, ORNL/TM-2019/1362, September 2019.
[47] D. Grabaskas, T. Fei, and J. Jerden, "Technical Letter Report on The Assessment of Tritium Detection and Control in Molten Salt Reactors: Final Report," Argonne National Laboratory, ANL/NSE-20-15, May 2020.
[48] D. O'Grady, T. Mui, A. Lee, L. Zou, G. Hu, and R. Hu, "SAM Code Enhancement, Validation, and Reference Model Development for Fluoride-salt-cooled High-temperature Reactors," Argonne National Laboratory, ANL/NSE-21/15, April 2021.
[49] C. Patricelli, "Analyzing fission product sample data from the Molten Salt Reactor Experiment," Argonne National Laboratory, Unpublished, 2021.
[50] E. L. Compere, E. G. Bohlmann, S. S. Kirslis, F. F. Blankenship, and G. W. R., "Fission Product Behavior in the Molten Salt Reactor Experiment," Oak Ridge National Laboratory, ORNL-4865 October 1975.
[51] J. Serp *et al.*, "The molten salt reactor (MSR) in generation IV: Overview and perspectives," *Progress in Nuclear Energy,* vol. 77, pp. 308-319, 2014.
[52] E. Merzari *et al.*, "Large-scale large eddy simulation of nuclear reactor flows: Issues and perspectives," *Nuclear Engineering and Design,* vol. 312, pp. 86-98, 2017.
[53] S. E. Beall, P. N. Haubenreich, R. B. Lindauer, and J. R. Tallackson, "MSRE Design and Operations Report. Part V. Reactor Safety Analysis Report," Oak Ridge National Laboratory, Oak Ridge, TN, 1964.
[54] B. Yamaji, A. Aszódi, M. Kovács, and G. Csom, "Thermal–hydraulic analyses and experimental modelling of MSFR," *Annals of Nuclear Energy,* vol. 64, pp. 457-471, 2014.
[55] M. R. Altahhan *et al.*, "Preliminary design and analysis of Liquid Fuel Molten Salt Reactor using multi-physics code GeN-Foam," *Nuclear Engineering and Design,* vol. 369, pp. 110826-110826, 2020.
[56] D. R. Shaver, L. B. Carasik, E. Merzari, N. Salpeter, and E. Blandford, "Calculation of Friction Factors and Nusselt Numbers for Twisted Elliptical Tube Heat Exchangers Using Nek5000," *Journal of Fluids Engineering,* vol. 141, no. 7, pp. 071205 (11 pages)-071205 (11 pages), 2019.
[57] H. Rouch *et al.*, "Preliminary thermal–hydraulic core design of the Molten Salt Fast Reactor (MSFR)," *Annals of Nuclear Energy,* vol. 64, pp. 449-456, 2014.
[58] A. T. Patera, "A spectral element method for fluid dynamics: Laminar flow in a channel expansion," *Journal of Computational Physics,* vol. 54, no. 3, pp. 468-488, 1984.
[59] L. W. Ho, "A Legendre spectral element method for simulation of incompressible unsteady viscous free-surface flows," 1989.

[60] G. Kalitzin, A. Gould, and J. Benton, "Application of two-equation turbulence models in aircraft design," (Aerospace Sciences Meetings: American Institute of Aeronautics and Astronautics, 1996.
[61] J. C. Kok and S. P. Spekreijse, "Efficient and accurate implementation of the k-omega turbulence model in the NLR multi-block Navier-Stokes system," National Aerospace Laboratory NLR, Netherlands, 2000.
[62] A. Tomboulides, S. M. Aithal, P. F. Fischer, E. Merzari, A. V. Obabko, and D. R. Shaver, "A novel numerical treatment of the near-wall regions in the k−ω class of RANS models," *International Journal of Heat and Fluid Flow,* vol. 72, pp. 186-199, 2018.
[63] A. Obabko, P. Fischer, O. Marin, E. Merzari, and D. Pointer, "Verification and Validation of Nek5000 for T-junction, Matis, SIBERIA, and Max Experiments," presented at the American Nuclear Society, Chicago, IL, 2015.
[64] G. Busco, E. Merzari, and Y. A. Hassan, "Invariant analysis of the Reynolds stress tensor for a nuclear fuel assembly with spacer grid and split type vanes," *International Journal of Heat and Fluid Flow,* vol. 77, pp. 144-156, 2019.
[65] P. Fischer and J. Mullen, "Filter-based stabilization of spectral element methods," *Comptes Rendus de l'Académie des Sciences - Series I - Mathematics,* vol. 332, no. 3, pp. 265-270, 2001.
[66] Y. Maday, A. T. Patera, and E. M. Rønquist, "An Operator-integration-factor splitting method for time-dependent problems: Application to incompressible fluid flow," *Journal of Scientific Computing,* vol. 5, no. 4, pp. 263-292, 1990.
[67] D. C. Wilcox, *Turbulence modeling for CFD*. DCW industries La Canada, CA, 1998.
[68] J. Fang *et al.*, "Feasibility of Full-Core Pin Resolved CFD Simulations of Small Modular Reactor with Momentum Sources," *Nuclear Engineering and Design,* vol. 378, pp. 111143-111143, 2021.
[69] C. Geuzaine and J.-F. Remacle, "Gmsh: A 3-D finite element mesh generator with built-in pre- and post-processing facilities," *International Journal for Numerical Methods in Engineering,* vol. 79, no. 11, pp. 1309-1331, 2009.
[70] V. C. Leite, D. Reger, J. Fang, H. Yuan, and D. Shaver, "Initial use of Nek5000/Cardinal to improve closure models in Pronghorn," Lemont, IL, 2021.
[71] Y. S. Jung, J. Fang, D. Shaver, and B. Feng, "Multi-Physics Simulations of Molten Chloride Fast Reactor using Nek5000 and PROTEUS-NODAL," Argonne National Laboratory, ANL/NSE-20/40, July 2020.
[72] R. Hu, "SAM Theory Manual," Argonne National Laboratory, ANL/NE-17/4, March 2017.
[73] D. de Wet, Oak Ridge National Laboratory, Unpublished Information, 2021.
[74] R. C. Steffy and P. J. Wood, "Theoretical Dynamic Analysis of the MSRE with U-233 Fuel," Oak Ridge National Laboratory, ORNL-TM-2571, July 1969.
[75] R. C. Steffy, "Experimental Dynamic Analysis of the MSRE with U-233 Fuel," Oak Ridge National Laboratory, ORNL-TM-2997, April 1970.
[76] M. Zanetti, A. Cammi, C. Fiorina, and L. Luzzi, "A Geometric Multiscale modelling approach to the analysis of MSR plant dynamics," *Progress in Nuclear Energy,* vol. 83, pp. 82-98, 2015.
[77] NRG, Personal Communication.

Nuclear Science and Engineering
Argonne National Laboratory
9700 South Cass Avenue, Bldg. 208
Argonne, IL 60439

www.anl.gov

Argonne National Laboratory is a U.S. Department of Energy laboratory managed by UChicago Argonne, LLC